Leprosy drug clofazimine activates peroxisome proliferator-activated receptor-γ and synergizes with imatinib to inhibit chronic myeloid leukemia cells

Harish Kumar,[1] Sourav Chattopadhyay,[1,2] Nabanita Das,[1] Sonal Shree,[3] Dinesh Patel,[4] Jogeswar Mohapatra,[4] Anagha Gurjar,[1,2] Sapana Kushwaha,[1] Abhishek Kumar Singh,[1] Shikha Dubey,[3] Kiran Lata,[3] Rajesh Kushwaha,[5] Riyazuddin Mohammed,[6] Krishnarup Ghosh Dastidar,[4] Namrata Yadav,[4] Achchhe Lal Vishwakarma,[7] Jiaur Rahaman Gayen,[6,2] Sanghamitra Bandyopadhyay,[5] Abhijit Chatterjee,[4] Mukul Rameshchandra Jain,[4] Anil Kumar Tripathi,[8] Arun Kumar Trivedi,[1,2] Naibedya Chattopadhyay,[9,2] Ravishankar Ramachandran[2,3] and Sabyasachi Sanyal[1,2]

[1]Division of Biochemistry, CSIR-Central Drug Research Institute, Lucknow; [2]AcSIR, CSIR-Central Drug Research Institute Campus, Lucknow; [3]Division of Molecular and Structural Biology, CSIR-Central Drug Research Institute, Lucknow; [4]Zydus Research Center, Moraiya, Ahmedabad, Gujarat; [5]Developmental Toxicology Laboratory, Systems Toxicology and Health Risk Assessment Group, CSIR-Indian Institute of Toxicology Research, Lucknow; [6]Pharmacokinetics and Metabolism Division, CSIR-Central Drug Research Institute, Lucknow; [7]Sophisticated Analytical Instrument Facility, CSIR-Central Drug Research Institute, Lucknow; [8]Department of Clinical Hematology and Medical Oncology, King George's Medical University, Lucknow, Uttar Pradesh and [9]Division of Endocrinology, CSIR-Central Drug Research Institute, Lucknow, India

 doi:10.3324/haematol.2018.194910

Received: April 11, 2019

Accepted: July 12, 2019.

Pre-published: August 1, 2019.

Correspondence: *SABYASACHI SANYAL* - sanyal@cdri.res.in

Supplemental Data: Kumar et al

Leprosy drug clofazimine activates peroxisome proliferator-activated receptor-γ and synergizes with imatinib to inhibit chronic myeloid leukemia cells

Harish Kumar[1], Sourav Chattopadhyay[1,2], Nabanita Das[1], Sonal Shree[3], Dinesh Patel[4], Jogeswar Mohapatra[4], Anagha Gurjar[1,2], Sapana Kushwaha[1], Abhishek Kumar Singh[1], Shikha Dubey[3], Kiran Lata[3], Rajesh Kushwaha[5], Riyazuddin Mohammed[6], Krishnarup Ghosh Dastidar[4], Namrata Yadav[4], Achchhe Lal Vishwakarma[7], Jiaur Rahaman Gayen[6,2], Sanghamitra Bandyopadhyay[5], Abhijit Chatterjee[4], Mukul Rameshchandra Jain[4], Anil Kumar Tripathi[8], Arun Kumar Trivedi[1,2], Naibedya Chattopadhyay[9,2], Ravishankar Ramachandran[2,3], Sabyasachi Sanyal[1,2]*

Supplemental methods:

Chemicals: Clofazimine and thiazolidinediones were from Sigma-Aldrich (St Louis, MO). Imatinib mesylate and dasatinib (used in *in vitro* experiments) were from Biovision. For *in vivo* experiments imatinib mesylate (Gleevec) was from Novartis (Novartis India LTD, Mumbai, India). Fine reagents were from Sigma-Aldrich and cell culture reagents were from Life Technologies (Thermo Fisher Scientific, Carlsbad, CA) unless otherwise indicated.

Antibodies and plasmids

Antibodies: phospho-STAT5, STAT5, phospho-ERK, T-ERK, Cleaved PARP and caspases -3,-8,-9, Bcl2, Bax, PRDX1, MYB, NF-κB p65, p105/50, c-Rel, PPAR-γ, Ubiquitin, ATF-4, CREB, E2F1, C-Jun, C-Fos, Phospho-c-Abl-Y245, Phospho-CrkL, Acetyl-Histone H3 (Lys9), Ki67 antibodies were from Cell Signaling Technology (Boston, MA). GR, PRDX2-5, Cytochrome C, Catalase, SOD1, NRF-2, c-Abl antibodies were from Santa Cruz Biotechnology (Santa Cruz, CA). SOD2/MnSOD, PDLIM2, CUL5, ING4 antibodies were from Abcam (Cambridge, MA). COMMD1 antibody was from Biorad (Hercules, CA). Anti-PRDX6 was from AbFrontier (Seoul, Korea). Mouse monoclonal anti-β-Actin-Peroxidase was from Sigma-Aldrich. Alexafluor-488 conjugated donkey anti-rabbit IgG (H+L) secondary antibody was from Molecular probes; Life Technologies. Peroxidase-conjugated IgG Fraction monoclonal mouse anti Rabbit IgG, Peroxidase-conjugated Affini Pure Goat Anti-Mouse IgG, (Light Chain Specific) were from Jackson Immuno Research Laboratories (West Grove, PA). Flow cytometry antibodies CD61-PE, CD34-PE and CD38-FITC were from BD Biosciences (East Rutherford, NJ) and CD41-FITC was from Biolegend (San

Diego, CA). For immunoblotting all primary antibodies were used in 1:1000 dilutions except β-actin (1: 50000). For flow cytometry manufacturer's instructions were followed.

Plasmids: pcDNA1.1-p65 FL was from Rune Toftgard (Department of Biosciences and Nutrition, Karolinska Institutet, Huddinge, Sweden**)**. MYB expression plasmid; pCI neo-hcM-HA[1] and 3 copy cMYB-RE-luc reporter; pGL4b-3XMRE(GG)-myc[2] were from Odd Stokke Gabrielsen (Department of Biosciences, University of Oslo, Norway). pCMV-HA-PRDX1[3] was from Chieko Kai (Laboratory Animal Research Center, The Institute of Medical Sciences, The University of Tokyo, Tokyo, Japan)**.** pGL2-cMYB promoter Luc[3] was from Miguel Campanero, (Department of Cancer Biology, Instituto de Investigaciones Biomedicas Alberto Sols, Consejo Superior de Investigaciones Científicas–Universidad Autónoma de Madrid, Madrid, Spain). pET28a- PPARγ-LBD[4] was from Giorgio Pochetti (CNR -Institute of Crystallography, Monterotondo Stazione, Rome, Italy). p-nuclear factor-κB (NFkB)-Luc was purchased from Agilent Technologies. Gal4-luc, pM PPAR-α/β/γ and 3X-DR-1-PPRE-Luc constructs used in this study are described earlier[5]. pCMX-mPPARγ-FL was a gift from David Mangelsdorf (University of Texas Southwestern Medical Center, Dallas, Texas). The PRDX1-Luc promoter (-1065-+83) cloned in PGL3-basic[6] was a kind gift from Kimitoshi Kohno (University of Occupational and Environmental Health, Kitakyushu, Japan). PRDX1-Luc deletion constructs were constructed by PCR and cloned in pGL3-basic vector. PCR was also performed to introduce mutations in Prdx1 promoter (-11 to +83). For construction of three copy MYB-RE corresponding to -11 to +9 sequence of the PRDX1 promoter (PRDX-MYB-RE), following oligonucleotides were annealed: 5'-TCAGGTACCCGTCCGTTCCGTCACGTCCGTTCCGTCACGTCCGTTCCGCTCGAGT TA-3' and 5'-TAACTCGAGCGGAACGGACGTGACGGAACGGACGTGACGGAACG GACGGGTACCTGA-3' and cloned into KpnI- XhoI sites of pGL3-promoter vector.

Cell viability, apoptosis and differentiation

Cell viability was assessed using CellTiter-Glo (Promega Madison, WI) or trypan blue exclusion cell counting. TUNEL assay for cells was performed using an APO-BrdU TUNEL Assay Kit (Thermo Fisher scientific) and TUNEL assay for tumor sections were conducted using an *In situ* cell death detection kit, TMR red (Roche) according to manufacturer's instructions. Apoptosis was assessed by Annexin V-FITC/APC kits (BD Biosciences and Biolegend respectively) using flow cytometry (FACSCalibur flow cytometer; Becton

Dickenson, San Jose, CA). Differentiation was assessed by light microscopy using Giemsa and May-Grünwald solution (Sigma) or by staining with CD41-FITC or CD61-PE antibodies followed by flow cytometry (FACSCalibur).

$CD34^+$ cells isolation and analysis of apoptosis

Cells from CML patients were first selected with anti-CD34 magnetic beads in a magnetic-activated cell sorter system using EasySep™ Human CD34 Positive Selection Kit (STEMCELL Technologies, Vancouver, Canada). Cells were then cultured in StemSpan SFEM II medium supplemented with Flt3L, SCF, IL-3, IL-6 and TPO (StemSpan $CD34^+$ Expansion Supplement). Isolated cells were then labeled with CD34-PE antibody (BD) and $CD34^+$ purity was determined in a FACSAria flow cytometer (Becton Dickenson, San Jose, CA). The observed purity was ≥80%. For assessing apoptosis in $CD34^+$ $CD38^+$ and $CD34^+$ $CD38^-$ subpopulations, $CD34^+$ cells were treated as indicated and then stained with PE-conjugated anti-CD34 and FITC-conjugated anti-CD38 antibodies for 30 min followed by incubation with Annexin V-APC/PI for 15 minutes and then were gated into $CD34^+38^+$ and $CD34^+38^-$ populations and apoptosis was assessed in a FACSAria flow cytometer. Aldehyde dehydrogenase activity was assessed using an Aldefluor kit (STEMCELL technologies) by flow cytometry (FACSCalibur).

CFSE assay

For assessing apoptosis in quiescent $CD34^+$ cells, purified $CD34^+$ cells were first stained with carboxyfluorescein succinimidyl ester (CFSE; Invitrogen) for 30 min. Cells were then washed and resuspended in SFEM medium supplemented with growth factors (as stated above) and were incubated at 37°C overnight. Next day, cells were treated as indicated in SFEM medium (with growth factors) and were maintained further for 4 days with supplementation of the drugs every 48h. Cells were then harvested, washed, and were labeled with CD34-PE and Annexin-APC antibodies and then gated into non-dividing cells ($CD34^+CFSE^{bright}$) and dividing cell ($CD34^+CFSE^{dim}$) population based on CFSE fluorescence intensity. Cells cultured in the presence of colchicine (100ng/ml; Sigma) were used to assess the range of CFSE fluorescence exhibited by cells that were undivided at the end of the culture time by using a FACSAria flow cytometer.

Colony forming assay:

To assess colony formation potential of cells, soft agar assay was used. In brief, purified $CD34^+$ cells were cultured in StemSpan SFEM II medium supplemented with Flt3L, SCF, IL-3, IL-6 and TPO (StemSpan $CD34^+$ Expansion Supplement) and treated with Vehicle, CFZ, imatinib or imatinib+CFZ for 4 days with supplementation of the drugs every 48h. For growth in soft agar (Invitrogen), treated $CD34^+$ cells (1000 cells) were cultured in SFEM medium (supplemented with above cytokines) containing 0.3% low-melting agarose (Top layer) on top of a 0.6% low-melting agarose (base layer) in 6-well plates for additional 4 weeks. The appeared colonies were observed under inverted microscope (Nikon Eclipse TS100) and colony number was counted by Image J software after staining with 0.005% (w/v) crystal violet.

Measurement of intracellular ROS levels:

Total ROS was determined by DCFDA (Sigma), total and mitochondrial superoxide were measured using DHE (Sigma) and Mitosox RED (Life Technologies). Mitochondrial membrane potential was assessed using JC-1 (Sigma). H_2O_2 was measured using an Amplex Red Kit (Invitrogen) in a FLUOstar Galaxy fluorimeter (BMG Labtech, Offenburg, Germany).

$CD34^+38^+$ and $CD34^+38^-$ sorting for RNA extraction and reverse transcription-PCR analysis

PBMCs were isolated on Percoll (Sigma) density gradient by centrifugation. For sorting the $CD34^-38^+$, $CD34^+38^+$ and $CD34^+38^-$ subpopulations, cells were stained with PE-conjugated anti-CD34 and FITC-conjugated anti-CD38 antibodies for 30 min and then were sorted using FACSAria flow cytometer and were collected in culture media. After collection, cells were washed in PBS and total RNA was extracted and QRT-PCR was performed as described below.

Transfections

HEK-293T was transfected using Lipofectamine LTX (Life Technologies). K562 transfections were carried out using Nucleofector kit V and a Nucleofector II device (Lonza; Rockland, ME). For RNA interference, 100nM human ON-TARGET plus siRNAs (Dharmacon; Thermo Fisher Scientific; Pittsburgh, PA) were transfected in K562 cells using

Nucleofector kit V. In all transfections efficiency of transfection was determined by GFP fluorescence (co-transfected eGFPC1 plasmid) and in luciferase assays GFP fluorescence was used for normalization.

Immunofluorescence and immunohistochemistry:

CP-CML cells were fixed for 30 min with 4% paraformaldehyde, permeabilized in PBS/0.3% BSA/0.5% Triton X-100 for 10min, and blocked with PBS/ 3% BSA. Cells were then incubated overnight with primary antibodies (1:250) and then with Alexafluor-488 conjugated secondary antibody (Molecular Probes, Thermo Fisher Scientific) and were analyzed by flow cytometry. For Ki67 staining of tumor sections, 5µm paraffin sections were deparaffinised and rehydrated followed by antigen retrieval using citrate buffer (pH6.0). The sections were then blocked with 3% BSA in 1X PBST for 1h and were incubated with Ki67 antibody (1:200) overnight at 4°C. The slides were then washed with PBS and were incubated with secondary antibody conjugated with Texas Red (1:500; Life Technologies) for 1 hour followed by mounting with fluoroshield mounting medium with DAPI (Abcam).

Ubiquitination assay

K562 cells were treated with 5µM CFZ for 1h and lysed in radioimmunoprecipitation assay buffer (25 mM Hepes, pH 7.5, 150 mM NaCl, 1% Triton-X-100, 10% Glycerol, 0.5mM DTT and 1mM Na_3VO_4) supplemented with 10mM N-ethylmaleimide, and protease inhibitor cocktails (Sigma). Protein lysates (700µg) were pre-cleared with protein-A agarose beads (Millipore) and IgG. Supernatants were incubated with 2µg anti-p65 antibody or IgG and 20µl protein-A agarose beads overnight at 4°C. Beads were washed and proteins were resolved by SDS-PAGE followed by immunoblotting. A peroxidase-conjugated AffiniPure Goat Anti-Mouse IgG, (Light Chain Specific) secondary antibody (Jackson Immunoresearch, West Grove, PA) was used in order to avoid detection of IgG heavy chain.

Lanthascreen assay

PPARγ competitive binding assay were carried out using a LanthaScreen TR-FRET Assay Kit (Invitrogen, Thermo Fisher Scientific) as per manufacturer's instructions.

Purification of PPARγ-LBD

The ligand binding domains of hPPARγ (193-475) was expressed as N-terminal His-tagged protein using a pET28a vector and purified as previously described[4]. Briefly, the plasmid was introduced in BL21 (DE3) *E coli* strain. Transformed colonies were grown overnight in LB media supplemented with 50µg/ml kanamycin at 37°C/180 rpm to an OD of 0.6. The culture was induced with 1mM IPTG at 30°C/140 rpm for 12-16 hrs. Bacterial cells were then harvested and resuspended in resuspension buffer (50 mM Tris pH-7.5, 200 mM NaCl, 10% glycerol, 1mM PMSF, 10mM imidazole). The sample was sonicated and centrifuged and collected supernatant was loaded on Ni-NTA agarose beads. Bound protein was washed with wash buffer 1 (50mM imidazole) and wash buffer 2 (80mM imidazole) and was eluted with 300mM imidazole. The quality of affinity-purified protein was then analyzed by 12% SDS-PAGE. The protein was further purified by Size-exclusion chromatography, where affinity-purified protein was loaded on Superdex 200 10/300 GL column for gel filtration. Column was pre-equilibrated with 50mM Tris-HCl pH7.5, 50mM NaCl. Void volume of column was 8.03ml. Elution of PPARγ-LBD was found to be at 15.97ml, which represented its monomeric nature in solution**.**

Isothermal titration calorimetry

Binding of CFZ with PPARγ-LBD was probed through ITC experiments using a VP-ITC instrument from Microcal (Malvern Instruments; Malvern, UK). Binding experiments were performed at pH 7.4 using 50 mM sodium phosphate and 50 mM NaCl supplemented with 2% DMSO. Purified protein was first dialyzed against the same buffer for the ITC experiments. PPARγ-LBD (50µM) was then placed in the sample cell (~ 1.43 ml). The concentration of CFZ and rosiglitazone used for titration were 5 times the protein concentration. 10µl aliquots of titrant solution were injected stepwise into the sample cell with 180s delay between two consecutive injections. All the titrations were performed at 37℃.

Surface Plasmon Resonance (SPR)

SPR was performed using a Biacore 3000 instrument (GE Healthcare). Anti-His antibody (Santa Cruz Biotech) was immobilized in one of the four flow cells on a CM5 sensor chip (Biacore) in 10 mM acetate, pH 5.0 using standard primary amine coupling chemistry at 8000 response unit density. We performed measurements at 25°C in 20 mM HEPES, pH 7.4, 150

mM NaCl and 0.8% DMSO. Binding using capturing molecule methodology was employed where 9nM his-tagged PPARγ-LBD was injected as capturing molecule. A dilution series of CFZ (0, 1, 2, 4, 8 &16μM) or pioglitazone (0, 0.5, 1, 2, 4 & 8μM) was injected over the captured his-tagged PPARγ-LBD for 180s at a flow rate of 30μl/min and the reactions were allowed to closely approach equilibrium. The binding response was measured for 150s after the end of injection. Following each injection cycle, chip surface was regenerated with two injections of 10mM Glycine pH 2.0. After subtracting the signal from the mock-coupled flow cell, sensograms were processed by BIA evaluation software (GE Healthcare) to obtain kinetic parameters of the interaction. The steady-state binding constants were determined by fitting the data to a 1:1 Langmuir isotherm as per the Biacore manual.

Western blotting:

Western blots were performed using previously published protocols[7,8]. Immunoreactivity was detected using a chemiluminescent HRP Substrate (Merck, Millipore, Billerica, MA) and in a LAS 4010 Chemi-doc Imager (GE Healthcare, Little Chalfont, UK).

Chromatinimmunoprecipitation (ChIP)

ChIP assay was performed using Kit (Merck, Millipore) according to manufacturer's protocol. Immunoprecipitated DNA was amplified using following oligonucleotide sequence: 5'-GAAAGCGCCGAGTCATTC-3' and 5'-GCCTTTATAGCCAGTAGGGATCT-3' for human PRDX1 promoter (-93-+83), 5'- AGCCACATCGCTCAGACAC-3' and 5'-GCCCAATACGACCAAATCC-3' for glyceraldehydes 3-phosphate dehydrogenase (GAPDH) and was quantified by real-time PCR using VeriQuest SYBR Green qPCR Master Mix (Affymetrix, Thermo Scientific) and LightCycler 480 System (Roche, Indianapolis, IN).

RNA extraction and reverse transcription-PCR analysis

Total RNA was extracted using TRI Reagent (Life Technologies (Carlsbad, CA) according to the manufacturer's recommendations. Total RNA (2μg) was reverse transcribed using High-Capacity cDNA Reverse Transcription Kit (Applied Biosystems; Foster City, CA). For KV1.3, cDNAs was amplified using the following primers: oligonucleotide sequences (5'-3') are: KV1.3-F- TGGTTCTCCTTCGAACTGCT, KV1.3-R CAATGCGATGGTCAAGACA C, GAPDH-F-GCAGGGGGGAGCCAAAAGGGT and GAPDH-R-TGGGTGGCAGTG ATGGCATGG. Quantitative real-time PCRs (QRT-PCR) were performed on a LightCycler 480 System (Roche, Indianapolis, IN) using VeriQuest SYBR Green qPCR Master Mix

(Affymetrix, Thermo Scientific). The QRT-PCR primers were designed using Universal Probe Library Assay Design Center (Roche Life Science) (sequences in **Supplemental Table S2**). The data were analyzed by ΔΔCT method with GAPDH or β-actin used as an internal control.

Murine xenograft model of human leukemia

Athymic nu/nu mice (10-12 weeks old) were issued from the animal breeding facility of Zydus Research Center (ZRC), registered under Rule 5(a) for the "Breeding and Experiments on Animals (control and supervision) rules 1998 (Registration no.77/1999 (CPCSEA)). All animal studies were conducted according to protocol which was reviewed and approved by the Institutional Animal Ethics Committee (IAEC) Protocol no. ZRC/PH/BP/002/07-2K18 in an AAALAC-accredited facility. Mice were inoculated subcutaneously in the right flank with 10 x 10^6 K562 cells in matrigel (BD Biosciences; San Jose, CA; 1:1 ratio). When tumors were palpable, mice were randomized into 4 groups using the Microsoft Excel randomization program. The no treatment control (vehicle; n=7) group received 0.5% methyl cellulose and the treatment groups received imatinib (50mg/kg; n=6), clofazimine (10mg/kg; n=6) and combination of both imatinib and clofazimine (50mg/kg, 10mg/kg respectively; n=6), orally once daily for 12 days. Mice were observed daily and body weights were measured every alternate day. Tumors were measured alternate day by a digital caliper to determine tumor volume using the formula V = ($Width^2$× Length)/2. Tumor growth was evaluated from the first day of treatment until day 13. At the end of the study, images were captured; tumors were resected and saved in formal saline for histological analysis and liver and spleen weights were taken.

Supplemental Table S1. Patient details. (CP; chronic phase, AP; accelerated phase, BC; blast crisis, FD; freshly diagnosed, Resistant; imatinib-resistant, Responder; imatinib-responder, ND; not detected, -; not done).

P-no.	Age/Gender	Stage of Disease	Categories	Mutation Test (IRMA)	Old Treatment	Current Treatment
P1	45/F	CP	Resistant	M351T	Imatinib	Tasigna
P2	32/M	CP	Responder	-	Imatinib	Imatinib/ Thalidomide refferred
P3	35/M	CP	Responder	-	Imatinib	Imatinib
P4	50/M	AP	FD	-		
P5	28/M	CP	Resistant	-	Imatinib	Imatinib/ Tasigna referred
P6	18/F	CP	Responder	-	Imatinib	Imatinib
P7	22/M	CP	Responder	-	Imatinib	Imatinib
P8	22/M	CP	FD	-		
P9	52/M	CP	Resistant	ND	Imatinib	Imatinib
P10	18/F	CP	Resistant	-	Imatinib	Imatinib 600mg
P11	40/F	CP	Resistant	-	Imatinib	Nilotinib 300mg
P12	15/M	CP	Responder	-	Imatinib	Imatinib
P13	43/M	CP	Responder	-	Imatinib	Imatinib
P14	30/M	CP	Responder	-	Imatinib	Imatinib
P15	27/F	CP	Responder	-	Imatinib	Imatinib
P16	30/M	CP	Responder	-	Imatinib	Imatinib
P17	52/M	CP	Resistant	ND	Imatinib	Tasigna
P18	22/F	CP	Resistant	ND	Imatinib	Tasigna
P19	31/F	CP	Resistant	-	Imatinib	Tasigna
P20	28/M	CP	Resistant	M351T	Imatinib	Sprycel 50mg
P21	60/F	CP	FD	-		
P22	25/M	CP	Resistant	Y253H	Imatinib	Sprycel 100mg
P23	29/M	CP	Resistant	ND	Imatinib	Tasigna
P24	60/F	BC	Responder	-	Imatinib	Imatinib
P25	50/F	CP	FD	-		
P26	23/M	CP	Resistant	F359V	Imatinib	Imatinib 600mg/Sprycel 100mg
P27	16/M	CP	Resistant	-	Imatinib	Imatinib

P28	28/F	CP	Resistant	-	Imatinib	Tasigna
P29	14/M	CP	FD	-		
P30	47/M	CP	Responder	-	Imatinib	Imatinib
P31	52/M	CP	Resistant	ND	Imatinib	Imatinib 600mg
P32	59/M	CP	FD	-	Imatinib	Imatinib
P33	18/M	CP	Resistant	ND	Imatinib	Imatinib 600mg/Tasigna referred
P34	50/M	CP	Responder	-	Imatinib	Imatinib
P35	43/M	CP	Resistant	ND	Imatinib	Tasigna/Sprycel 50mg
P36	25/M	CP	Responder	-	Imatinib	Imatinib
P37	22/M	CP	FD	-	Imatinib	Imatinib
P38	22/M	CP	Resistant	-	Imatinib	Imatinib/Hydroxy Urea
P39	47/M	CP	Resistant	-	Imatinib	Tasigna
P40	15/M	BC	Resistant	-	Imatinib	Tasigna
P41	45/M	CP	Resistant	-	Imatinib	Imatinib 600mg
P42	30/M	CP	Responder	-	Imatinib	Imatinib
P43	47/F	CP	Resistant	Y253H	Imatinib	Tasigna
P44	27/M	CP	Resistant	M244V	Imatinib	Imatinib 600mg
P45	36/F	CP	Resistant	M351T	Imatinib	Tasigna
P46	72/F	CP	Resistant	-	Imatinib	Tasigna
P47	50/M	CP	Responder	-	Imatinib	Imatinib
P48	35/F	CP	Responder	-	Imatinib	Imatinib
P49	24/F	CP	Responder	-	Imatinib	Imatinib
P50	55/M	CP	Responder	-	Imatinib	Imatinib
P51	38/F	CP	Resistant	-	Imatinib	Tasigna
P52	40/F	CP	Responder	-	Imatinib	Imatinib
P53	38/F	CP	responder	-	Imatinib	Imatinib
P54	30/F	CP	Resistant	-	Imatinib	Tasigna
P55	38/M	CP	Resistant	-	Imatinib	Imatinib 600mg
P56	38/M	CP	Responder	-	Imatinib	Imatinib
P57	40/F	CP	Responder	-	Imatinib	Imatinib
P58	38/F	CP	Responder	-	Imatinib	Imatinib
P59	35/M	CP	Responder	-	Imatinib	Imatinib
P60	42/M	CP	Resistant	-	Imatinib	Tasigna
P61	41/M	CP	Resistant	G250E	Imatinib	Tasigna
P62	45/M	CP	Resistant	ND	Imatinib	Imatinib 600mg failure/Tasigna referred

P63	36/F	CP	Resistant	-	Imatinib	Imatinib 600mg/ Sprycel 100mg referred
P64	45/M	CP	Resistant	-	Imatinib	Tasigna
P65	40/M	CP	Resistant	ND	Imatinib	Imatinib 600mg
P66	28/F	CP	Resistant	-	Imatinib	Imatinib 600mg
P67	26/F	CP	Responder	-	Imatinib	Imatinib
P68	56/M	CP	Responder	-	Imatinib	Imatinib
P69	38/F	CP	Resistant	M351T	Imatinib	Tasigna
P70	35/F	CP	Resistant	-	Imatinib	Imatinib/Sprycel 100mg
P71	41/F	AP	Resistant	-	Imatinib	Tasigna
P72	41/F	CP	Resistant	ND	Imatinib	Nilotinib 200mg
P73	35/M	BC	Resistant	-	Imatinib	Sprycel 100mg
P74	29/M	CP	Resistant	ND	Imatinib	Tasigna
P75	28/M	CP	Resistant	ND	Imatinib	Tasigna
P76	40/M	CP	Resistant	ND	Imatinib	Imatinib/Tasigna referred
P77	35/M	CP	Resistant	-	Imatinib	Imatinib/Tasigna referred
P78	36/F	BC	Resistant	-	Imatinib	Imatinib/Tasigna & Sprycel referred
P79	29/M	CP	Resistant	ND	Imatinib	Tasigna
P80	42/M	CP	Resistant	ND	Imatinib	Tasigna
P81	35/F	CP	Resistant	ND	Imatinib	Imatinib 600mg
P82	28/F	CP	Resistant	ND	Imatinib	Tasigna
P83	80/M	CP	Resistant	ND	Imatinib	Hydrea 500mg
P84	29/M	CP	Resistant	ND	Imatinib	Tasigna
P85	47/F	CP	Resistant	Y253H	Imatinib	Tasigna
P86	28/F	CP	Resistant	ND	Imatinib	Imatinib 600mg
P87	34/M	CP	Resistant	H396R/M224V	Imatinib	Spycel 50mg/ Tasigna
P88	49/F	CP	Resistant	L387M/M351T	Imatinib	Dasatinib 100mg
P89	45/F	CP	Responder	-	Imatinib	Imatinib
P90	50/M	CP	Responder	-	Imatinib	Imatinib
P91	36/F	CP	Resistant	M351T	Imatinib	Tasigna

P92	74/M	CP	FD	-		
P93	38/M	CP	Responder	-	Imatinib	Imatinib
P94	56/M	CP	Resistant	ND	Imatinib	Imatinib
P95	55/F	CP	Resistant	-	Imatinib	Tasigna

Supplemental Table S2. Oligonucleotide sequences used for QRT-PCR. h; human. All sequence in 5'-3' orientation.

Gene name	Genbank Accession number	Forward primer	Reverse primer
hNF-κB-p65	NM_021975.3	CGGGATGGCTTCTATGAGG	GGATGCGCTGACTGATAGC
hPRDX1	NM_001202431.1	GGTTGCAGTAAGCCAACACC	CCTGAAGACATCTTCCTATCAGC
hMYB	NM_001130173.1	AGCAAGGTGCATGATCGTC	GATCACACCATGATGAAGAATCAG
hPPAR-γ	NM_005037.5	GACAGGAAAGACAACAGACAAATC	GGGGTGATGTGTTTGAACTTG
hSTAT-5B	NM_012448.3	TGAAGGCCACCATCATCAG	TGTTCAAGATCTCGCCACTG
hHIF-1α	NM_001243084.1	TTTTTCAAGCAGTAGGAATTGGA	GTGATGTAGTAGCTGCATGATCG
hHIF-2α	NM_001430.4	GACAGAATCACAGAACTGATTGGT	CGCATGGTAGAATTCATAGGC
hCITED-2	NM_001168389.1	TCACTTTCAAGTTGGCTGTCC	CATTCCACACCCTATTATCATCTGT
hBCL-2	NM_000633.2	CGACGACTTCTCCCGCCGCTACCGC	CCGCATGCTGGGGCCGTACAGTTCC
hGAPDH	NM_001289746.1	AGCCACATCGCTCAGACAC	GCCCAATACGACCAAATCC
hβ-actin	NM_001101.5	AGAGCTACGAGCTGCCTGAC	CGTGGATGCCACAGGACT

Supplemental Table S3: CFZ and imatinib combination; ATP-based cell survival assay followed by Compusyn analysis. CI; combination index.

CFZ (μM)	IMT (μM)	Effect	CI
1.56	0.0001	0.44	0.058
1.56	0.001	0.38	0.030
1.56	0.01	0.22	0.006
1.56	0.1	0.19	0.019
1.56	0.25	0.18	0.037
1.56	0.5	0.17	0.061
1.56	1	0.15	0.079
1.56	1.56	0.15	0.123
1.56	3.12	0.14	0.196
1.56	6.25	0.13	0.308
1.56	12.5	0.12	0.476
1.56	25	0.09	0.385

Supplemental Table S4: Pioglitazone and imatinib combination; ATP-based cell survival assay followed by Compusyn analysis. CI; combination index.

Pio (μM)	IMT (μM)	Effect	CI
10	0.0001	0.80	0.154
10	0.001	0.72	0.109
10	0.01	0.60	0.251
10	0.1	0.55	1.60
10	0.25	0.42	1.33
10	0.5	0.22	0.370
10	1	0.10	0.105
10	2.5	0.09	0.206
10	5	0.06	0.165
10	10	0.06	0.330
10	25	0.05	0.551
10	50	0.03	0.361
10	100	0.03	0.723

Supplemental Table S5: CFZ and dasatinib combination; ATP-based cell survival assay followed by Compusyn analysis. CI; combination index.

CFZ (μM)	Dasa (μM)	Effect	CI
1.56	0.001	0.62	0.485
1.56	0.01	0.54	0.248
1.56	0.1	0.27	0.051
1.56	0.25	0.24	0.081
1.56	0.5	0.19	0.079
1.56	1	0.16	0.097
1.56	1.56	0.15	0.126
1.56	3.12	0.14	0.208
1.56	6.25	0.07	0.069
1.56	12.5	0.06	0.095
1.56	25	0.04	0.070

Figure S1

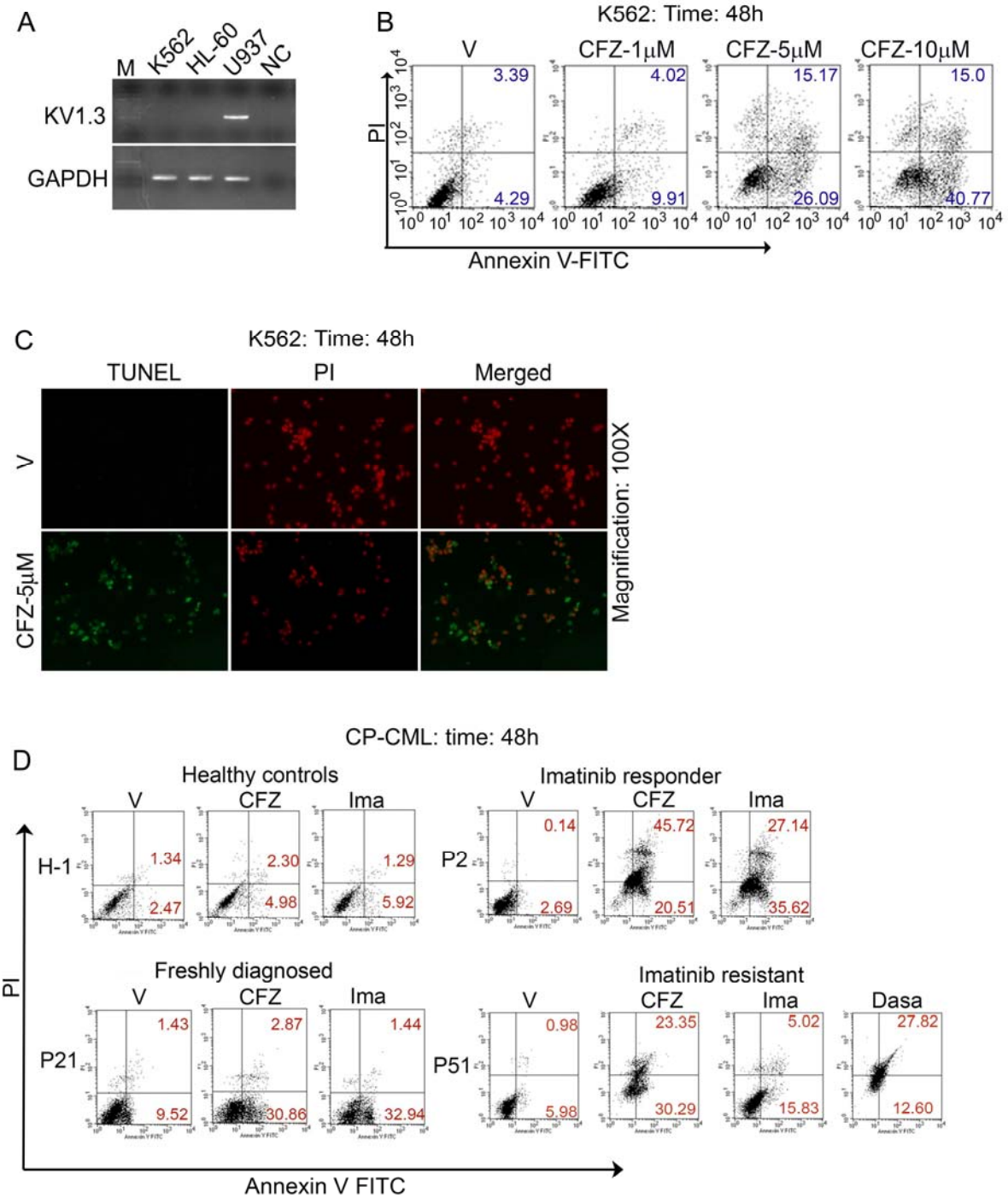

Supplemental Figure S1. CFZ induces apoptosis in K562 and CP-CML cells. (**A**) K562 cells do not express KV1.3 potassium channel. Reverse-transcriptase PCR-based detection of KV1.3 in leukemia cell lines. M; DNA ladder, NC; no DNA control. Data is representative of three independent experiments. (**B**) K562 cells were treated with indicated concentrations of CFZ and apoptosis was assessed by Annexin V/PI staining. Representative dot plot corresponding to **Figure 1B**. (**C**) determination of apoptosis in K562 in response to CFZ by TUNEL staining (Objective 10X, microscope: AxioImager M2, Carl Zeiss). Images representative of two independent experiments (8 fields/group). (**D**) CFZ induces apoptosis in CP-CML cells (all drugs 5μM). Representative dot plots corresponding to **Figure 1E**.

Figure S2

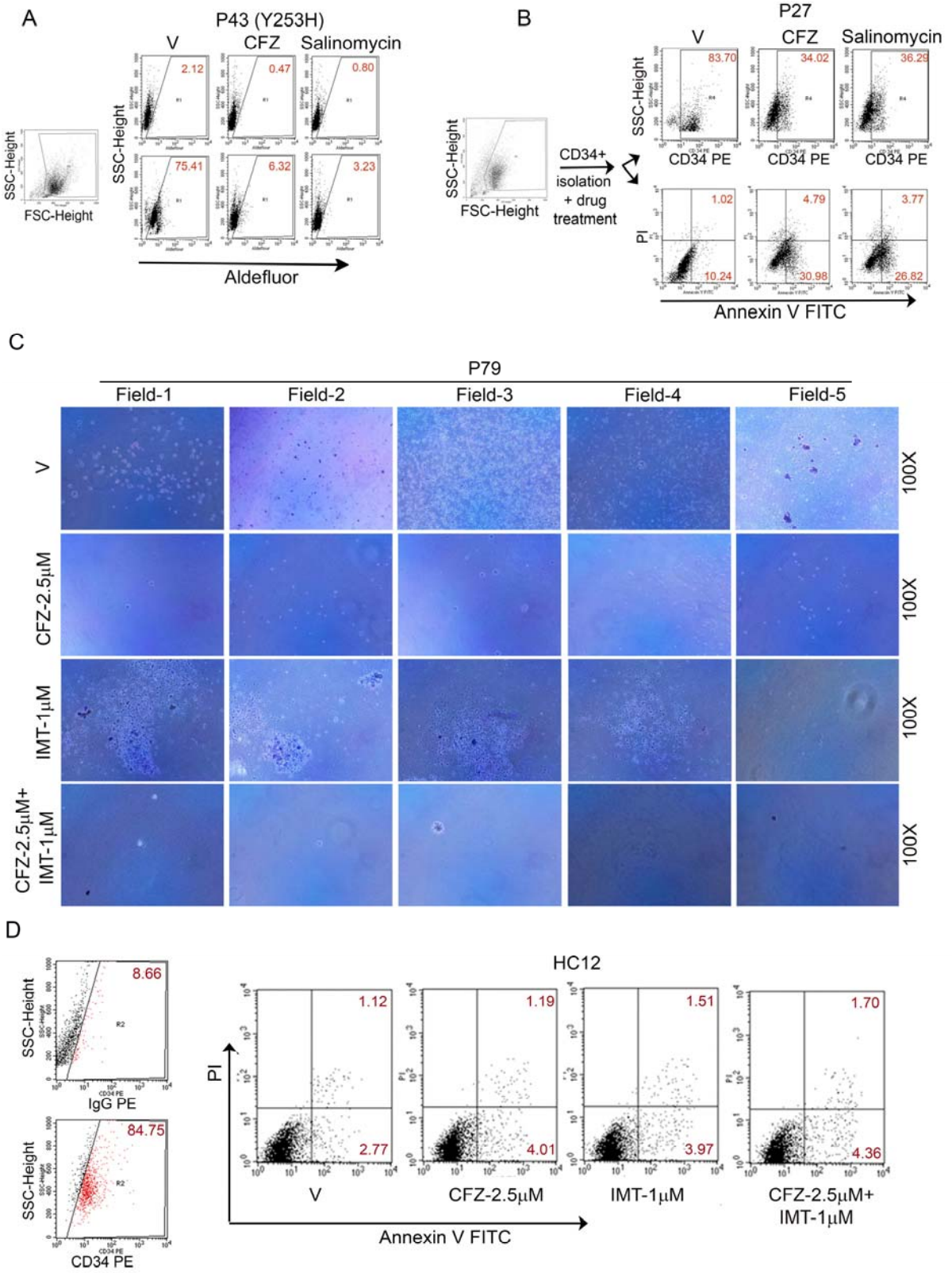

Supplemental Figure S2. CFZ reduces LSC load. (A) CFZ inhibits aldehyde dehydrogenase activity in CP-CML cells. CP-CML cells from imatinib-resistant patients were treated with CFZ or salinomycin (5μM; 48h) and aldehyde dehydrogenase activity in

these cells were assessed using an ALDEFLUOR kit (Stemcell technologies). Sets of experiments using aldehyde dehydrogenase inhibitor diethylaminobenzaldehyde (DEAB) was used as negative control. Representative dot plots corresponding to **Figure 1G** (n=6). (**B**) $CD34^+$ cells from imatinib-resistant patients (n=3) were isolated using a CD34 microbead kit (Miltenyi Biotech) and were treated with 5μM CFZ or salinomycin for 48h. Cells were then divided into two groups. One group was assessed by immunostaining for CD34 (**upper panel**) and the other group was stained with annexin V/PI (**lower panel**) and the cells were then analyzed by flow-cytometry (representative dot plot corresponding to **Figure 1I)**. (**C**) CFZ alone or in combination with imatinib reduces colony forming cells (n=3, total 15 images/treatment group, 5 fields from one patient sample is shown). Images correspond to **Figure 1H**. (**D**) Clofazimine alone or in combination with imatinib does not induce apoptosis in $CD34^+$ cells from healthy controls. Purified $CD34^+$ cells from healthy controls were treated as indicated for 48h and apoptosis was evaluated by Annexin V staining (representative dot plot corresponding to **Figure 1L** is shown).

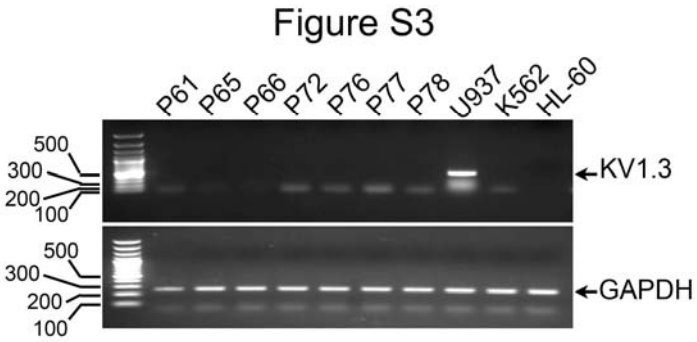

Supplemental Figure S3. $CD34^+$ CP-CML cells do not express KV1.3 transcript. Total RNA was isolated from indicated samples and reverse transcribed. Following which the indicated transcripts were detected by PCR and 1.5% agarose gel electrophoresis.

Figure S4

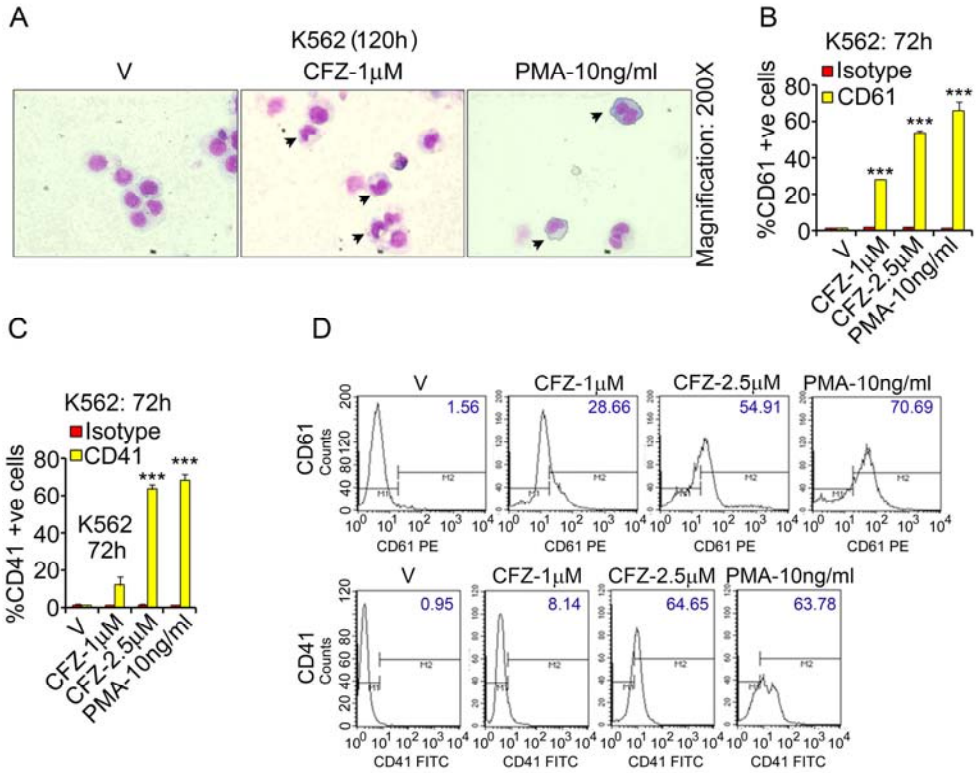
A
K562 (120h)
V
CFZ-1μM
PMA-10ng/ml
Magnification: 200X
B
K562: 72h
Isotype
CD61
%CD61 +ve cells
***
V
CFZ-1μM
CFZ-2.5μM
PMA-10ng/ml
C
K562: 72h
Isotype
CD41
%CD41 +ve cells
K562
72h
D
V
CFZ-1μM
CFZ-2.5μM
PMA-10ng/ml
1.56
28.66
54.91
70.69
CD61 Counts
CD61 PE
0.95
8.14
64.65
63.78
CD41 Counts
CD41 FITC
E
Freshly diagnosed
P4 (AP)
Imatinib responder
P34
Imatinib resistant
P39
V
CFZ
Isotype SSC-Height
CD61 SSC-Height
0.35
0.38
1.78
38.15
3.69
3.53
12.33
43.78
1.73
1.91
1.38
51.01
CD61 PE
F
Imatinib resistant
P9
Isotype SSC-Height
CD41 SSC-Height
1.89
2.00
1.60
68.31
CD41 FITC
G
V
CFZ
Mag: 400X, scale bar 25μm
H
CD34+ cells
P84
P82
SSC-height
IgG PE
2.90
CD34 PE
83.08
Isotype Counts
CD61 Counts
1.47
3.22
7
45.78
CD61 PE
CD11b Counts
1.05
2.79
2.5
56.7
CD11b PE

Supplemental Figure S4. **CFZ induces differentiation in K562, CP-CML and CP-CML CD34$^+$ cells at sublethal concentrations.** (**A**) CFZ induces megakaryocytic phenotype (Objective 20X, microscope: AxioImager M2, Carl Zeiss) data representative of two independent experiments (8fields/treatment group). (**B-D**) CFZ induces expression of megakaryocyte surface markers CD61 and CD41 in K562 cells. K562 cells were treated as indicated and were evaluated for CD61 (**B**), CD41 (**C**) expressions by flow cytometry (n=3). (**D**) Representative histograms. (**E**) CP-CML cells from freshly diagnosed, imatinib responders, and imatinib-resistant patients were treated with 1μM CFZ for 72h and cells were then stained CD61 antibodies and were analyzed by flow cytometry. (**F**) CP-CML cells from imatinib-resistant patients were treated with CFZ (1μM; 72h) and CD41 expression was determined by flow cytometry. (**E-F**) representative dot plots corresponding to **Figure 1M**. (**G**). CD34$^+$ cells isolated from CML patients were treated with CFZ (1μM; 120h; in absence of cytokine cocktail) and were analyzed by May-Grünwald-Giemsa staining. Images correspond to Figure 1N. (**H**) CFZ induces CD61 and CD11b expression in CD34$^+$ cells from CML patients. Cells were treated with 1μM CFZ for 72h and CD61 and CD11b expression was determined by flow cytometry. Representative histograms corresponding to Figure 1O-P. AP; accelerated phase.

Figure S5

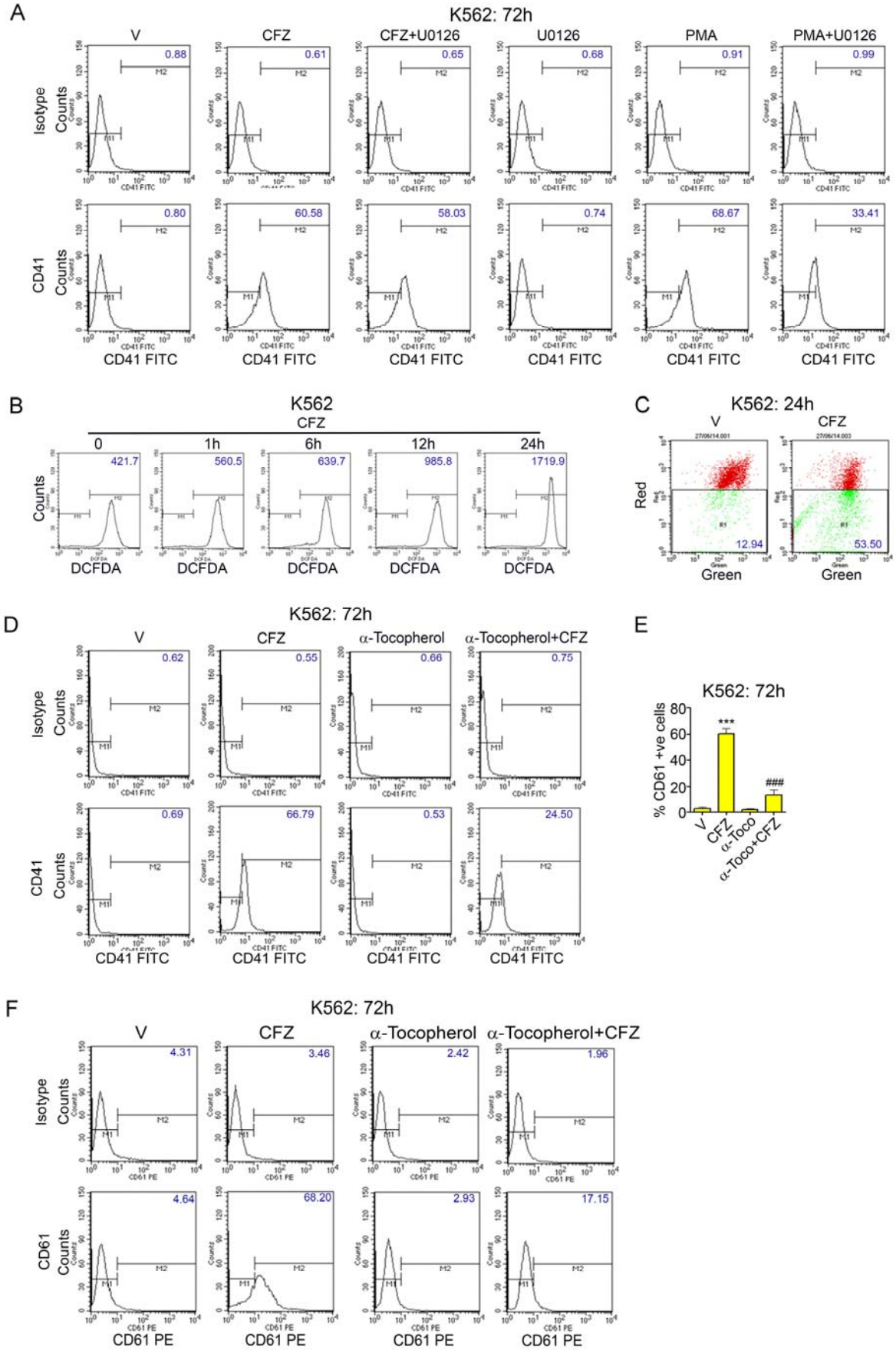
A
K562: 72h
V
CFZ
CFZ+U0126
U0126
PMA
PMA+U0126
Isotype Counts
CD41 Counts
0.88
0.61
0.65
0.68
0.91
0.99
0.80
60.58
58.03
0.74
68.67
33.41
CD41 FITC
B
K562
CFZ
0
1h
6h
12h
24h
421.7
560.5
639.7
985.8
1719.9
Counts
DCFDA
C
K562: 24h
V
CFZ
Red
Green
12.94
53.50
D
K562: 72h
V
CFZ
α-Tocopherol
α-Tocopherol+CFZ
Isotype Counts
CD41 Counts
0.62
0.55
0.66
0.75
0.69
66.79
0.53
24.50
CD41 FITC
E
K562: 72h
% CD61 +ve cells
***
###
V
CFZ
α-Toco
α-Toco+CFZ
F
K562: 72h
V
CFZ
α-Tocopherol
α-Tocopherol+CFZ
Isotype Counts
CD61 Counts
4.31
3.46
2.42
1.96
4.64
68.20
2.93
17.15
CD61 PE

Supplemental Figure S5. **CFZ induces megakaryocytic differentiation markers via enhancement of cellular ROS.** (**A**) MEK inhibitor U0126 fails to inhibit CFZ-induced CD41 expression. K562 cells were treated with CFZ (2.5μM) or PMA (10ng/ml) alone or in combination with 10μM U0126 for 72h. Cells were then stained with IgG1 isotype control or CD41 IgG1 antibodies and were analyzed by flow cytometry. Representative histogram corresponding to **Figure 2A.** (**B**) CFZ induces cellular ROS production. K562 cells were treated with 5μM CFZ for indicated time periods and were then stained with DCFDA and analyzed by flow cytometry. Representative histogram corresponding to **Figure 2C.** (**C**) CFZ induces mitochondrial membrane depolarization. K562 cells were treated with 5μM CFZ for 24h and mitochondrial membrane potential was determined using JC-1 staining followed by flow cytometry. Representative histogram corresponding to **Figure 2G.** (**D**) α-Tocopherol mitigates CFZ-induced increase in cell surface CD41 expression. K562 cells were treated with CFZ (2.5μM) or α-Tocopherol (200μM) alone or in combination for 72h and CD41 expression was evaluated by flow cytometry. Representative histogram corresponding to **Figure 2I**. (**E-F**) α-Tocopherol mitigates CFZ-induced increase in cell surface CD61 expression. Experiments were conducted as above (**D**) and CD61 expression was analyzed by flow cytometry. (**E**) Data from three independent experiments were plotted (Mean ± SEM). Data was analyzed by one-way ANOVA followed by Bonferroni's post-test. ***,$^{\#\#\#}$p<0.0001. *Comparison with vehicle-treated group. $^{\#}$Comparison with CFZ group. (**F**) Representative histograms.

Figure S6

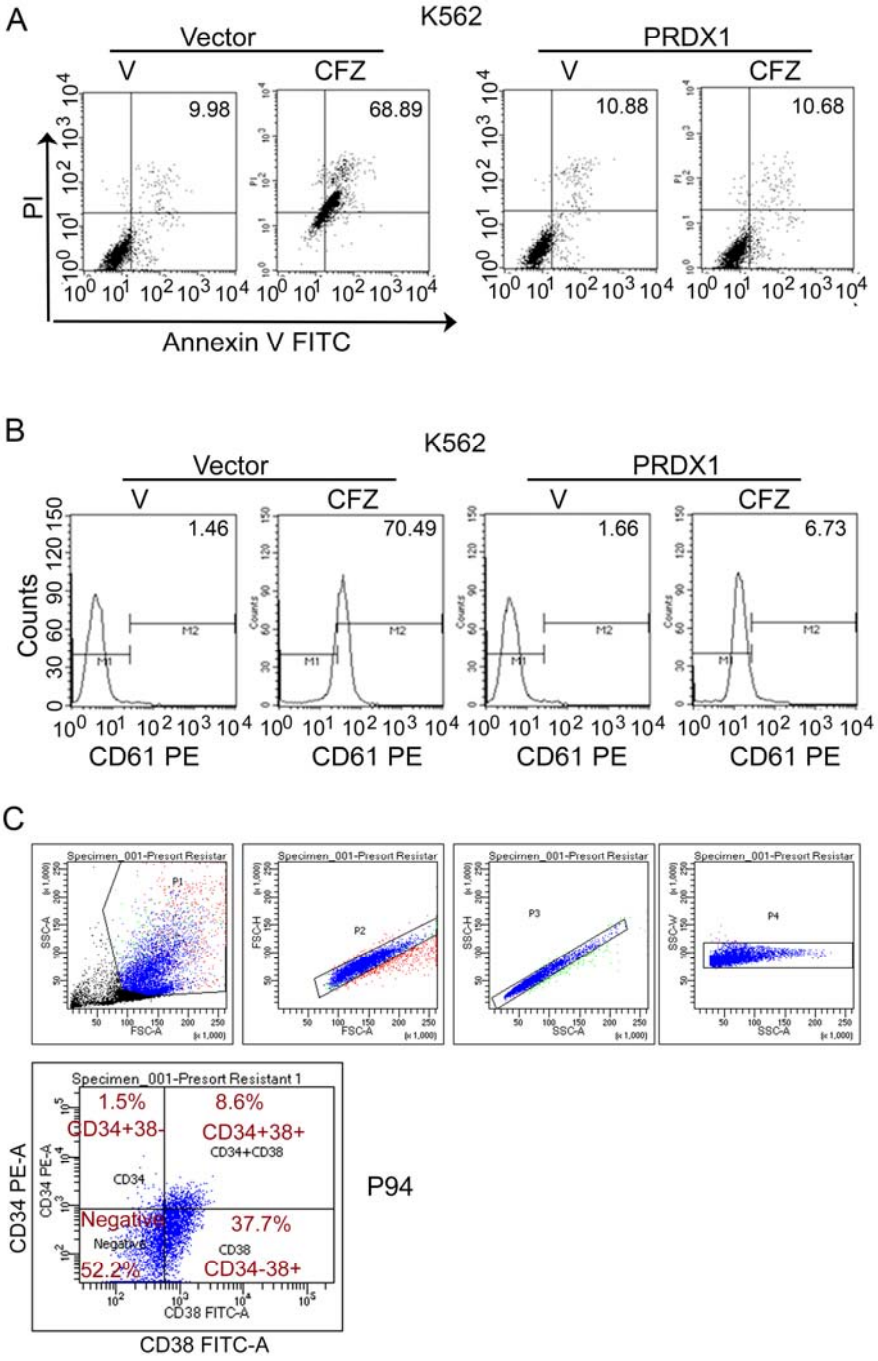

Supplemental Figure S6. **CFZ-dependent apoptosis and differentiation in K562 cells is alleviated by PRDX1 overexpression**. (**A**) Exogenous PRDX1 mitigates CFZ-induced apoptosis. K562 cells were transfected with PRDX1 or corresponding empty vector and were treated with 5μM CFZ for 48h. Cells were then stained with Annexin V/PI and analyzed by flow cytometry. Representative dot plots of one from three independent experiments are shown. Data corresponds to **Figure 3C.** (**B**) Exogenous PRDX1 mitigates CFZ-induced K562 differentiation. K562 cells were transfected with PRDX1 or corresponding empty vector and were treated with 2.5μM CFZ for 72h. Cells were then stained with CD61 antibody and analyzed by flow cytometry. Representative histograms of one from three independent

experiments are shown. Data represents **Figure 3D**. (**C**) Flow cytometry based sorting of $CD34^{+}38^{+}$ and $CD34^{+}38^{-}$cells for determination of PRDX1 mRNA expression. One representative data corresponding to **Figure 3J** is shown.

Figure S7

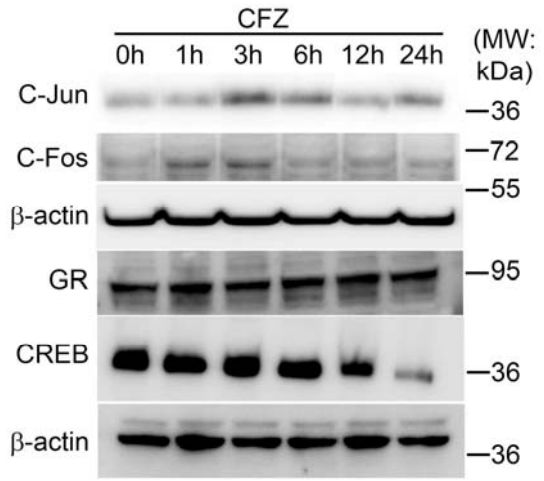

Supplemental Figure S7. Effect of CFZ on expression of various proteins in K562 cells. K562 cells were treated with 5μM CFZ for indicated time periods. Cells were then lysed and expression of indicated proteins was evaluated by western blotting. One representative of three independent experiments is shown.

Figure S8

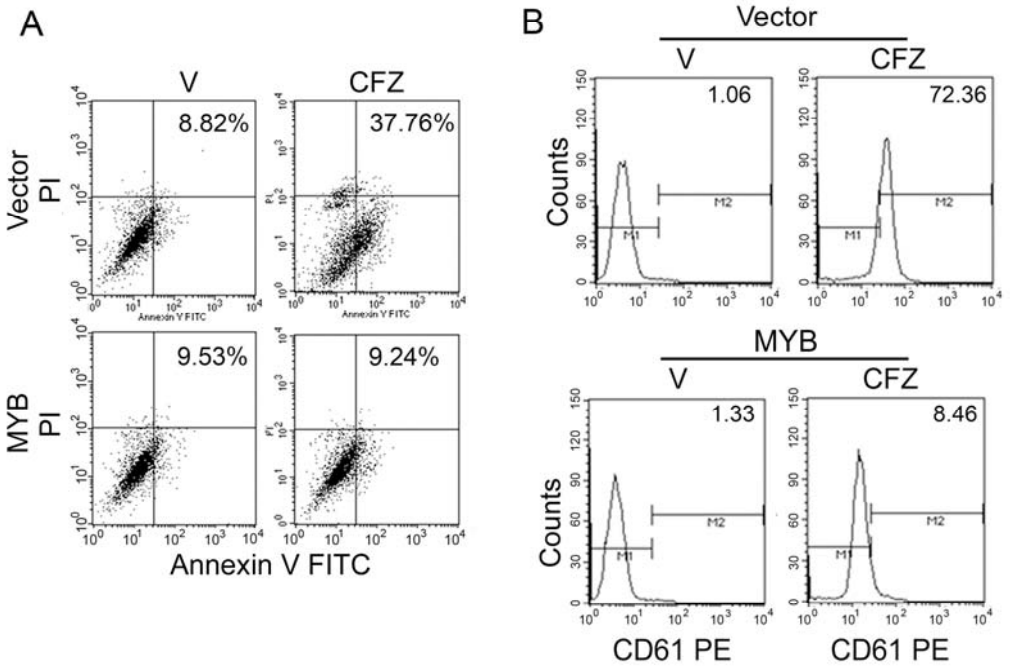

Supplemental Figure S8. Exogenous MYB mitigates CFZ-induced apoptosis and differentiation in K562 cells. (**A-B**) K562 cells were transfected with MYB expression plasmid or corresponding empty vectors. (**A**) 24h after transfection cells were treated with vehicle or CFZ (5μM) for 48h and apoptosis was assessed by Annexin/PI staining followed by flow cytometry. (**B**) 24h after transfection, cells were treated with vehicle or 2.5μM CFZ for 72h. Cells were then stained with CD61 antibodies and analyzed by flow cytometry. Representative dot plots or histograms from three independent experiments are shown. Data correspond to **Figure 4M** and **N** respectively.

Figure S9

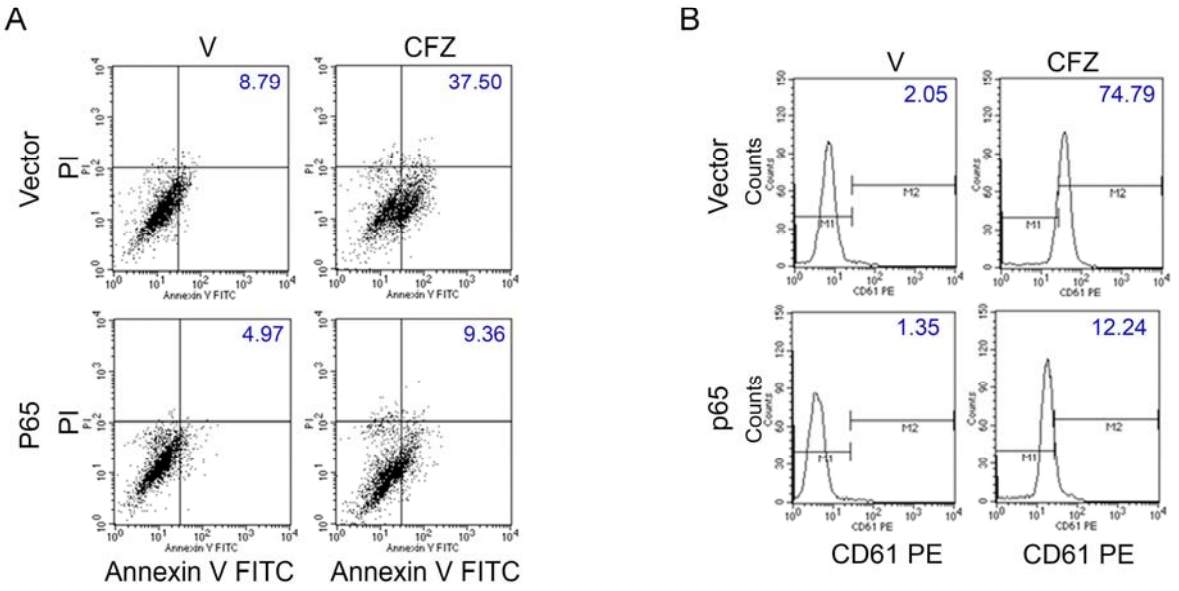

Supplemental Figure S9. Exogenous p65 mitigates CFZ-induced apoptosis and differentiation in K562 cells. (**A-B**) K562 cells were transfected with p65 expression plasmid or corresponding empty vectors. (**A**) 24h after transfection cells were treated with vehicle or CFZ (5μM) for 48h and apoptosis was assessed by Annexin/PI staining followed by flow cytometry. (**B**) 24h after transfection, cells were treated with vehicle or 2.5μM CFZ for 72h. Cells were then stained with CD61 antibodies and analyzed by flow cytometry. Representative dot plots or histograms from three independent experiments are shown. Data correspond to **Figure 5I** and **J** respectively.

Figure S10

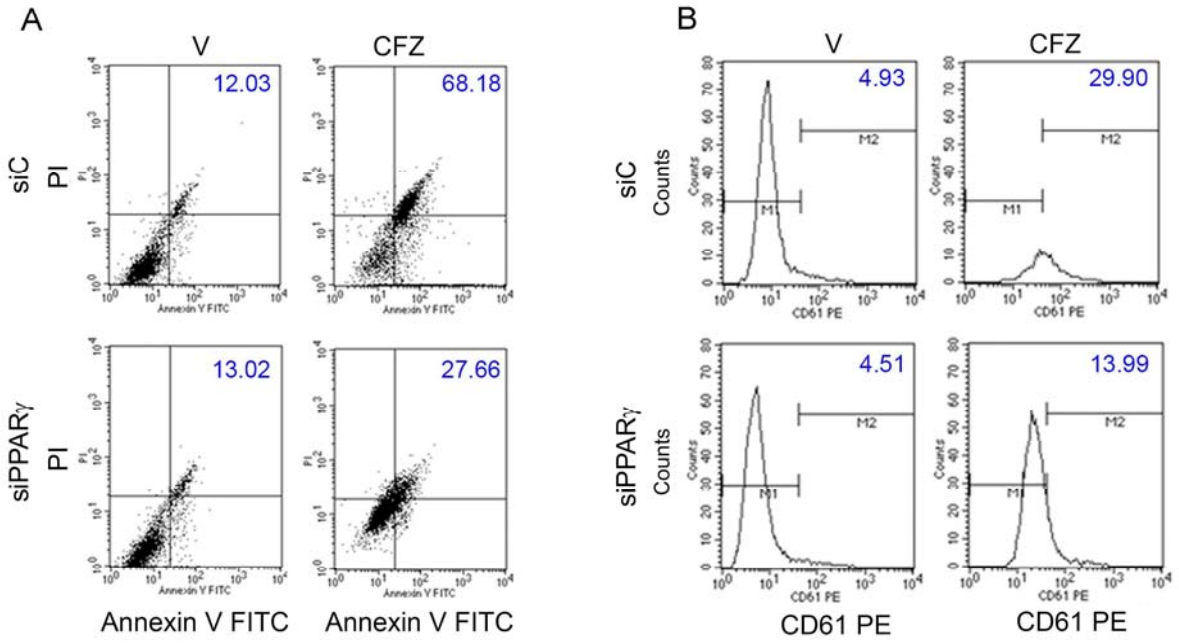

Supplemental Figure S10. Depletion of PPARγ mitigates CFZ-induced apoptosis and differentiation in K562 cells. (**A-B**) K562 cells were transfected with siPPARγ or a non-silencing control siRNA (PGL3). (**A**) 48h after transfection cells were treated with vehicle or CFZ (5μM) for 48h and apoptosis was assessed by Annexin/PI staining followed by flow cytometry. (**B**) 48h after transfection, cells were treated with vehicle or 2.5μM CFZ for 72h. Cells were then stained with CD61 antibodies and analyzed by flow cytometry. Representative dot plots or histograms from three independent experiments are shown. Data correspond to **Figure 6C** and **D** respectively.

Figure S11

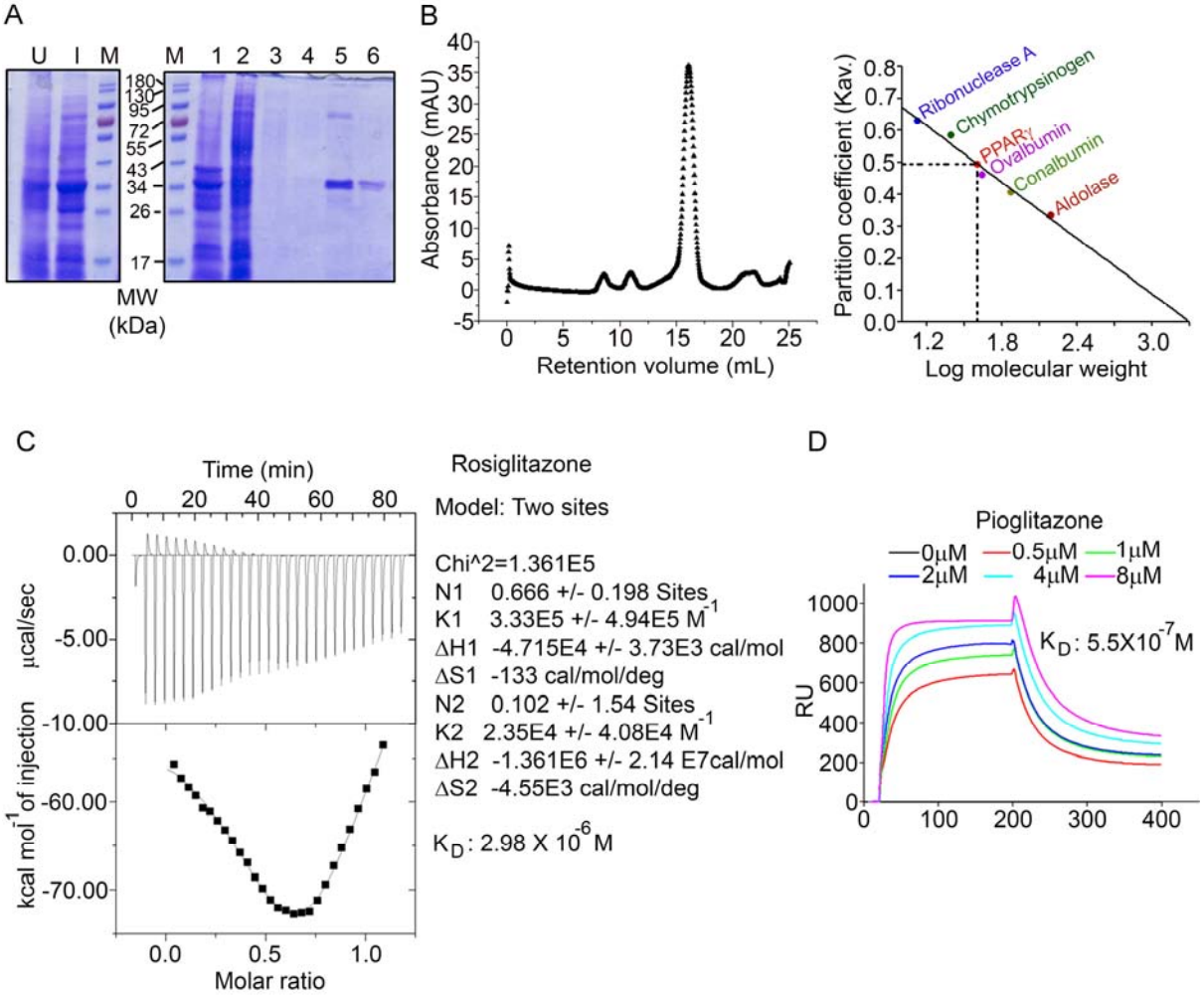

Supplemental Fig. S11. Production, purification and characterization of PPARγ-LBD. (A) Overexpression and purification of PPARγ-LBD. Lane U: uninduced sample, lane 1: induced sample (1mM IPTG), lane M: protein marker, lane1: supernatant, Lane2: flow-through, lane3: wash with 50mM imidazole, lane4: wash with 80mM imidazole, lane5: elution of PPARγ-LBD, Lane6: homogenous protein fraction of PPARγ-LBD after size-exclusion chromatography. (**B**) Gel elution profile of PPARγ-LBD**.** Size-exclusion chromatography of PPARγ-LBD was performed with Superdex200 10/300 GLOBAL column (GE). The chromatogram depicted monomeric form of PPARγ-LBD eluted at 15.97mL. (**C**) Isothermal titration calorimetry experiment of rosiglitazone with PPARγ-LBD. Rosiglitazone (250 µM) was titrated into PPARγ-LBD solution (50µM). The typical isotherm was found to be exothermic with stoichiometry of two i.e., two molecules of rosiglitazone binds with one PPAR gamma macromolecule. The K_D value was calculated to 2.98 µM. (**D**) SPR sensogram curve depicting interaction between the indicated concentrations of Pioglitazone and 6X-His tagged PPARγ-LBD captured over anti-His antibody immobilized CM5 chip. The K_D was determined to be 0.55µM**.**

Figure S12

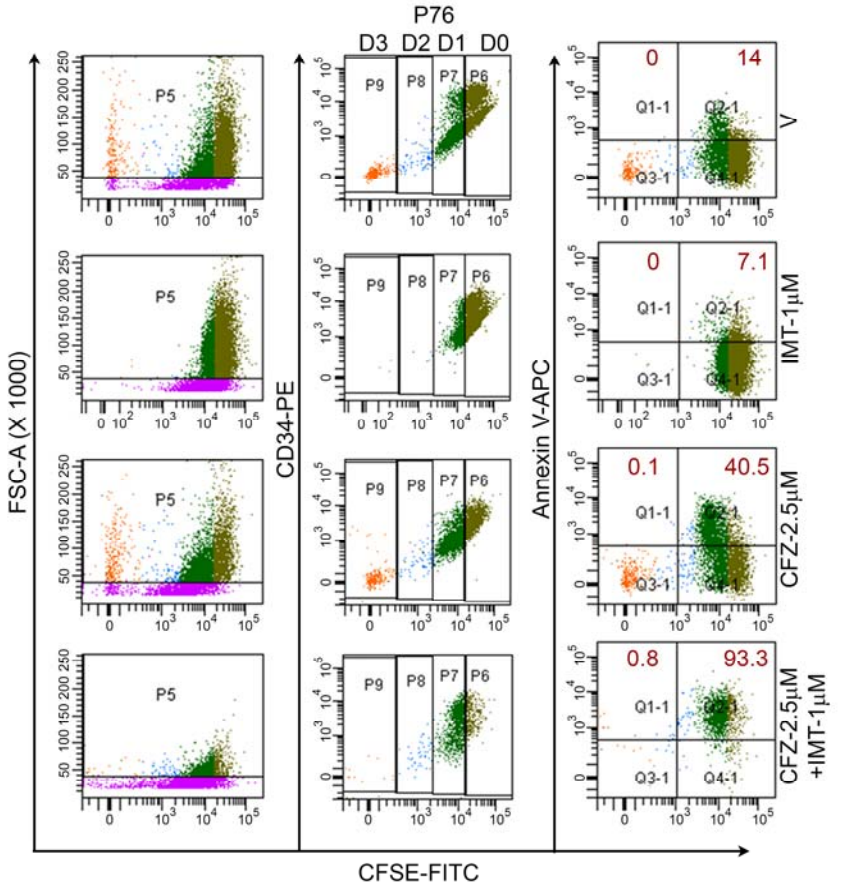

P76
% Cells

	D3	D2	D1	D0
V	2.84	0.65	32.50	64.01
IMT	0.02	0.04	19.89	80.05
CFZ	4.66	1.79	58.78	34.77
CFZ+IMT	0.62	2.34	74.70	22.34

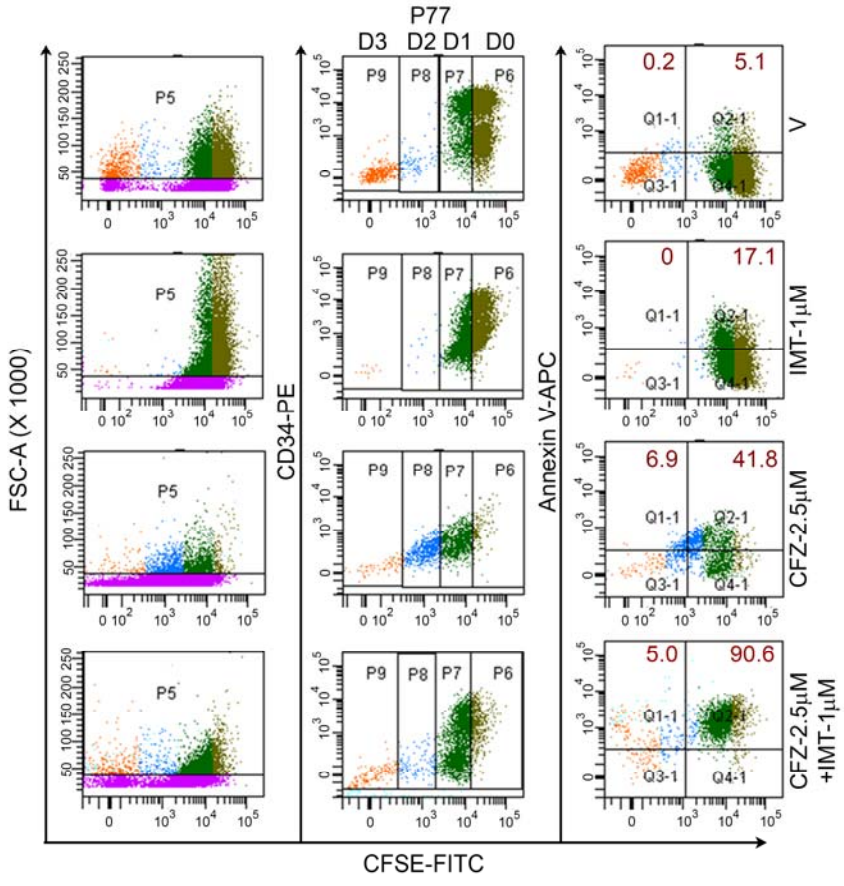

P77
% Cells

	D3	D2	D1	D0
V	5.58	0.85	24.11	69.45
IMT	0.09	0.17	35.06	64.68
CFZ	4.41	34.60	52.48	8.51
CFZ+IMT	4.68	3.43	76.60	15.28

Supplemental Figure S12. CFZ alone or in combination with IMT reduces quiescent CD34$^+$ population and induces apoptosis in these cells. CD34$^+$ population from imatinib-resistant CP-CML cells was purified by percoll density gradient centrifugation and CD34$^+$ selection via magnetic bead–based separation. CD34$^+$ cells were labeled with 2μM CFSE and were treated as indicated for 96h. Cells were gated depending on CFSE intensity. Distribution (%) of CFSE/CD34$^+$cells in each cell division is shown in different colored dots (D0-D3 represent cell division number). Apoptosis in these cells was determined by APC-labeled annexin V staining followed by flow-cytometry (FACSAria, BD biosciences). Data corresponds to **Figure 7J-L.**

Figure S13

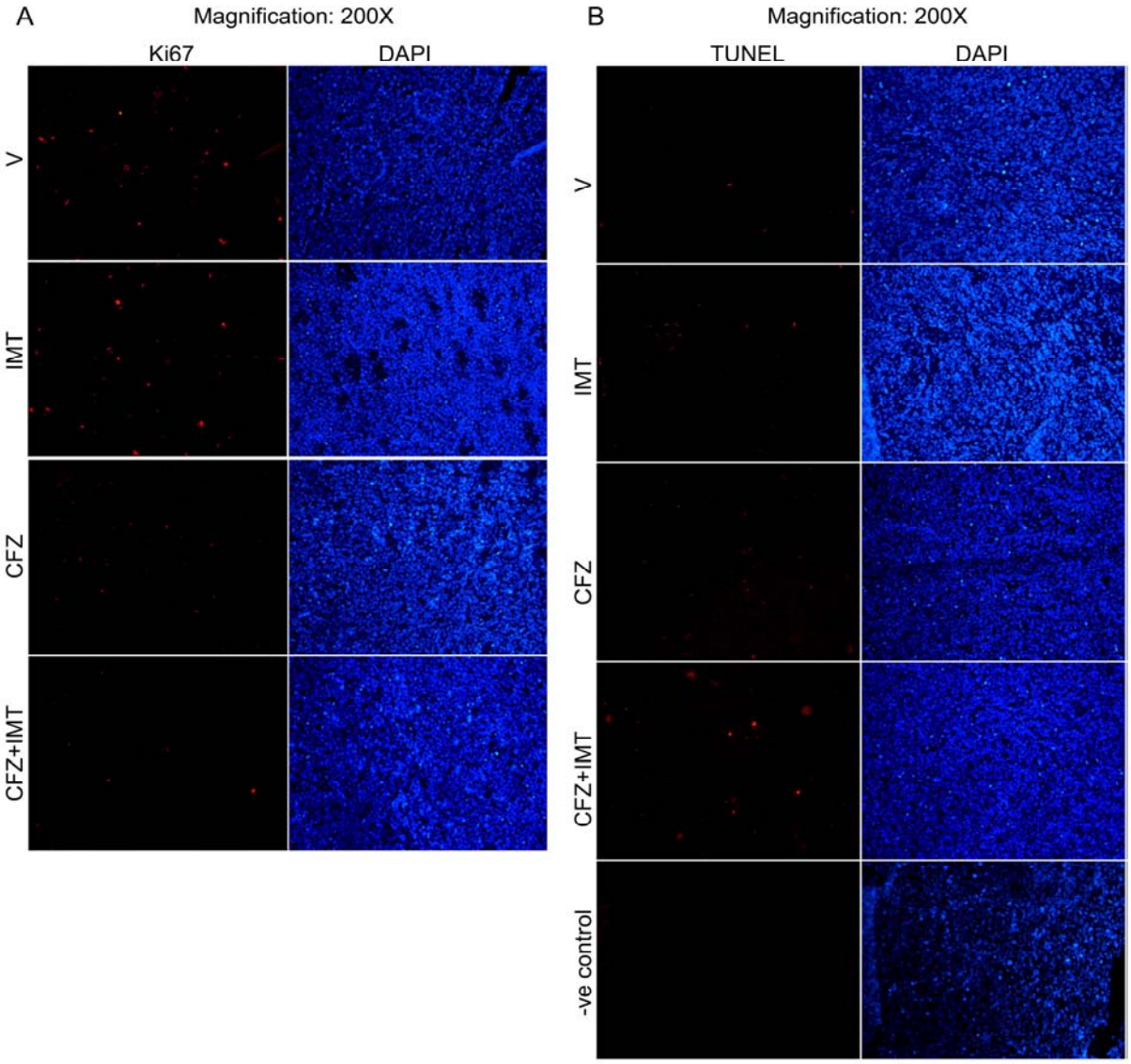

Supplemental Figure S13. A. Ki67 staining. B. TUNEL staining of tumor sections. Original images corresponding to **Figure 8F and H** respectively.

Figure S14 (full blots: Fig.1)

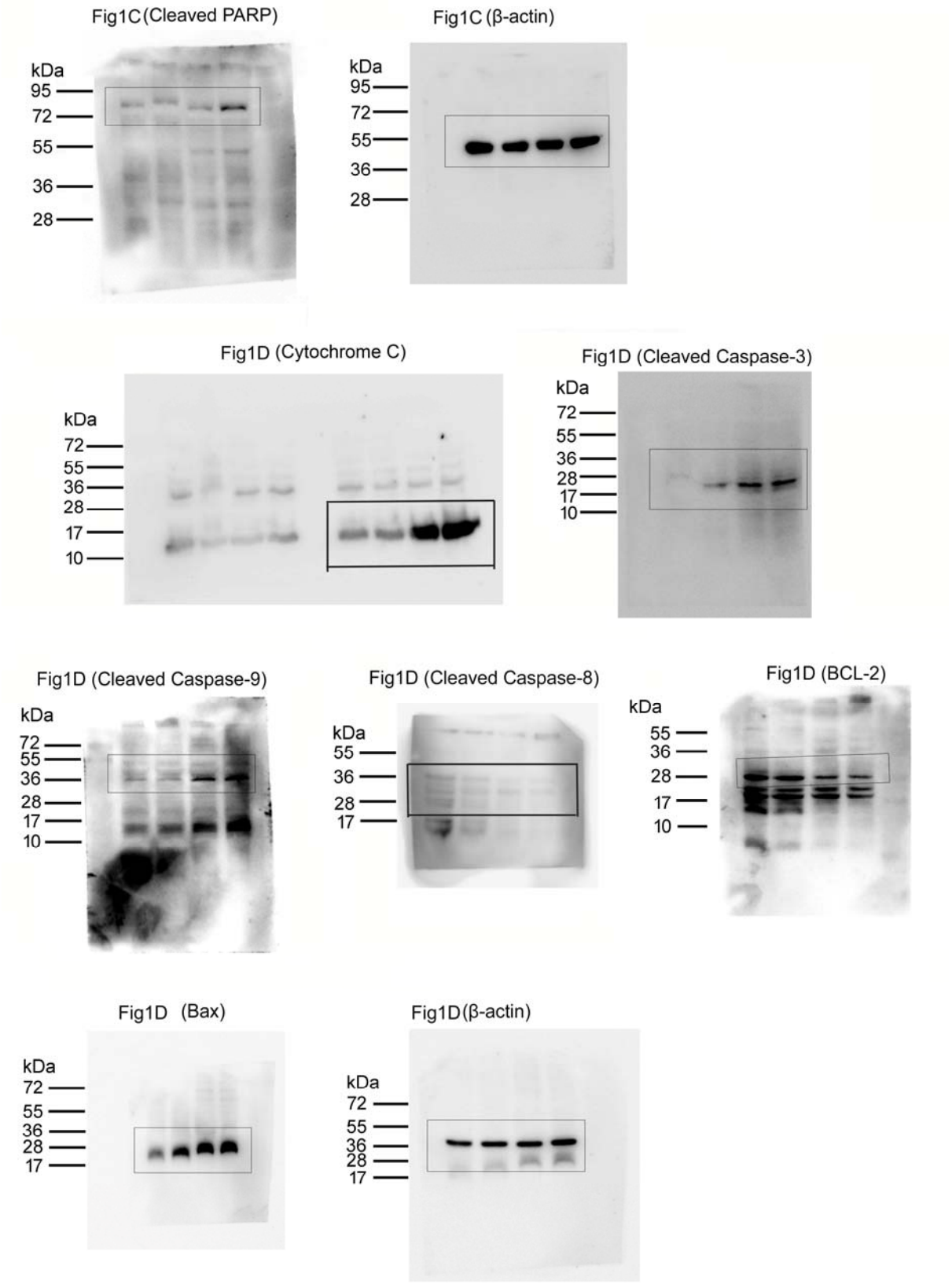

Figure S14 (full blots: Fig.2)

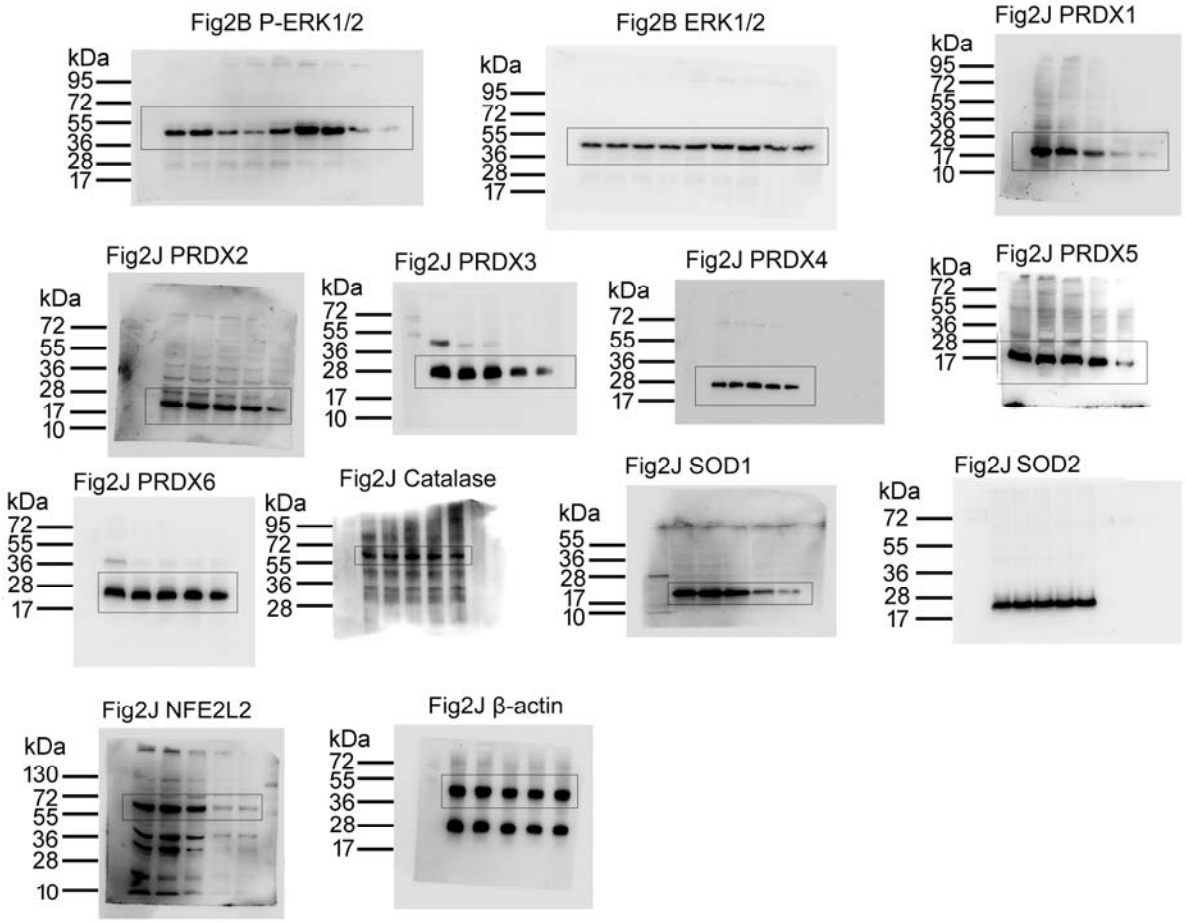

Figure S14 (full blots Fig: 3)

Fig 3B PRDX1

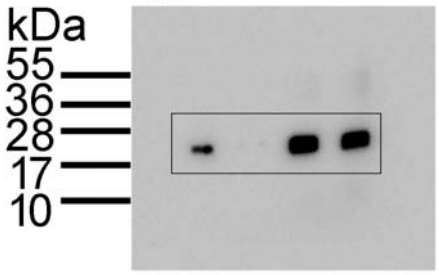

Fig3B Cleaved Caspase-3

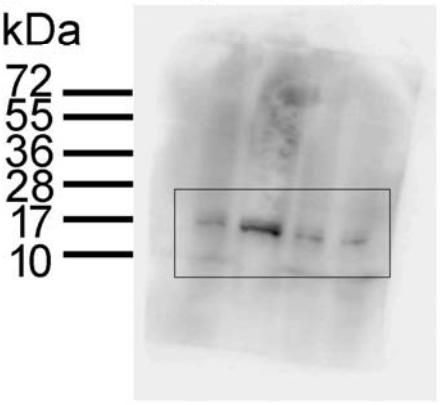

Fig3B Cleaved Caspase-9

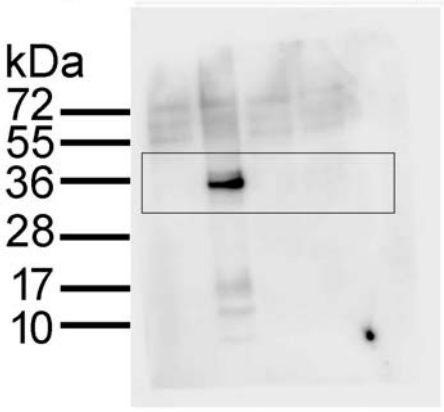

Fig 3B Bax

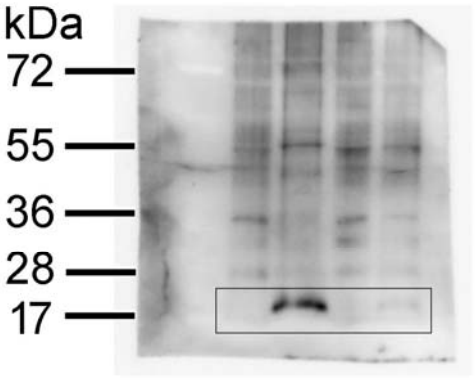

Fig3B β-actin

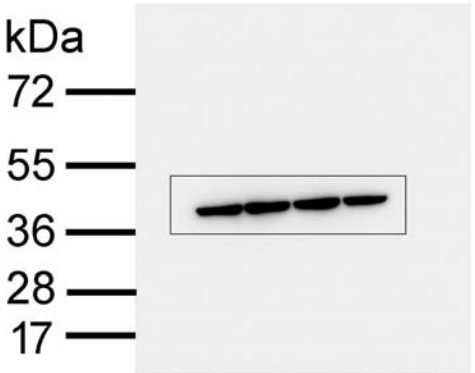

Figure S14 (Full blots: Fig 4)

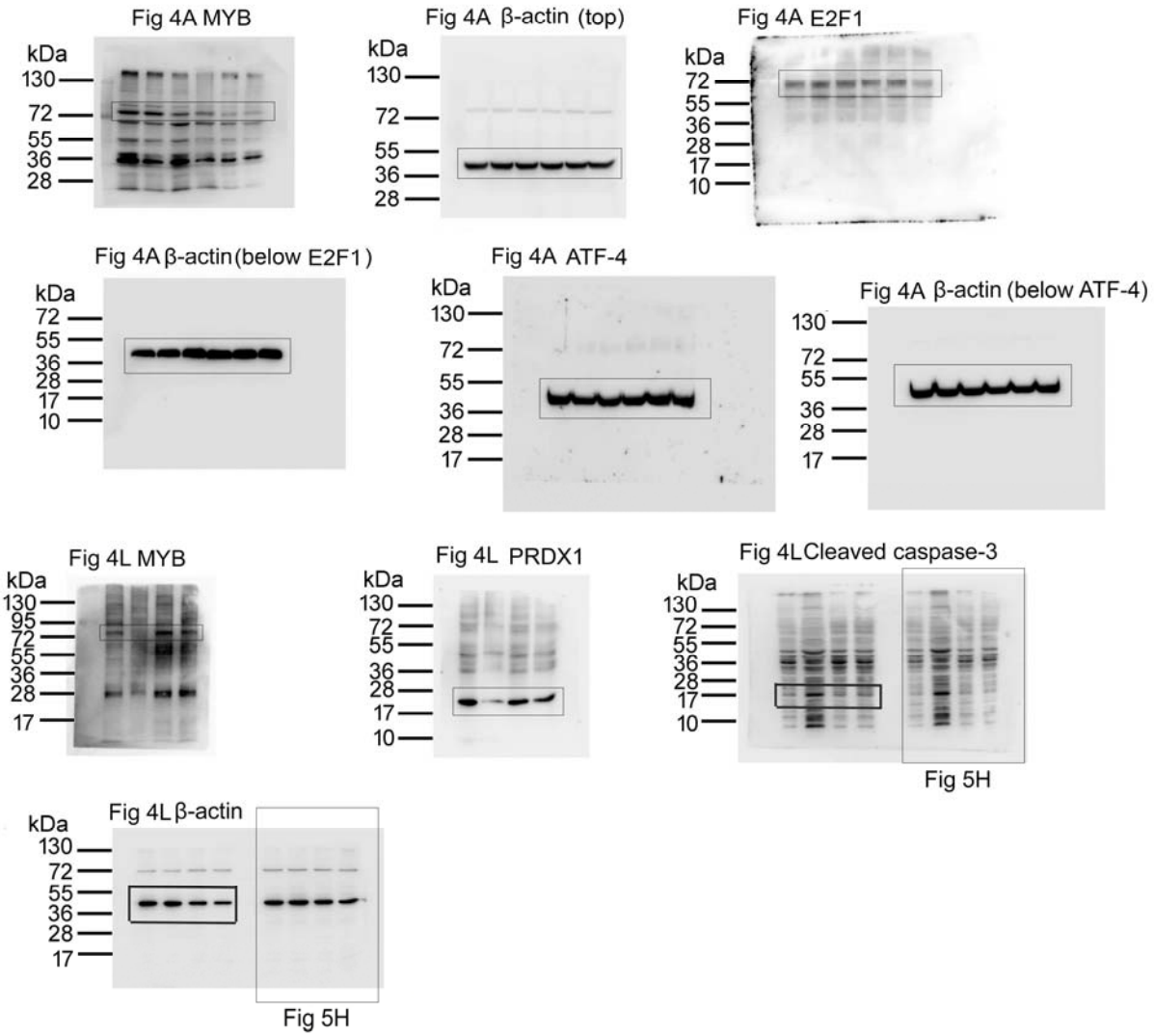

Figure S14 (Full blots: Fig 5)

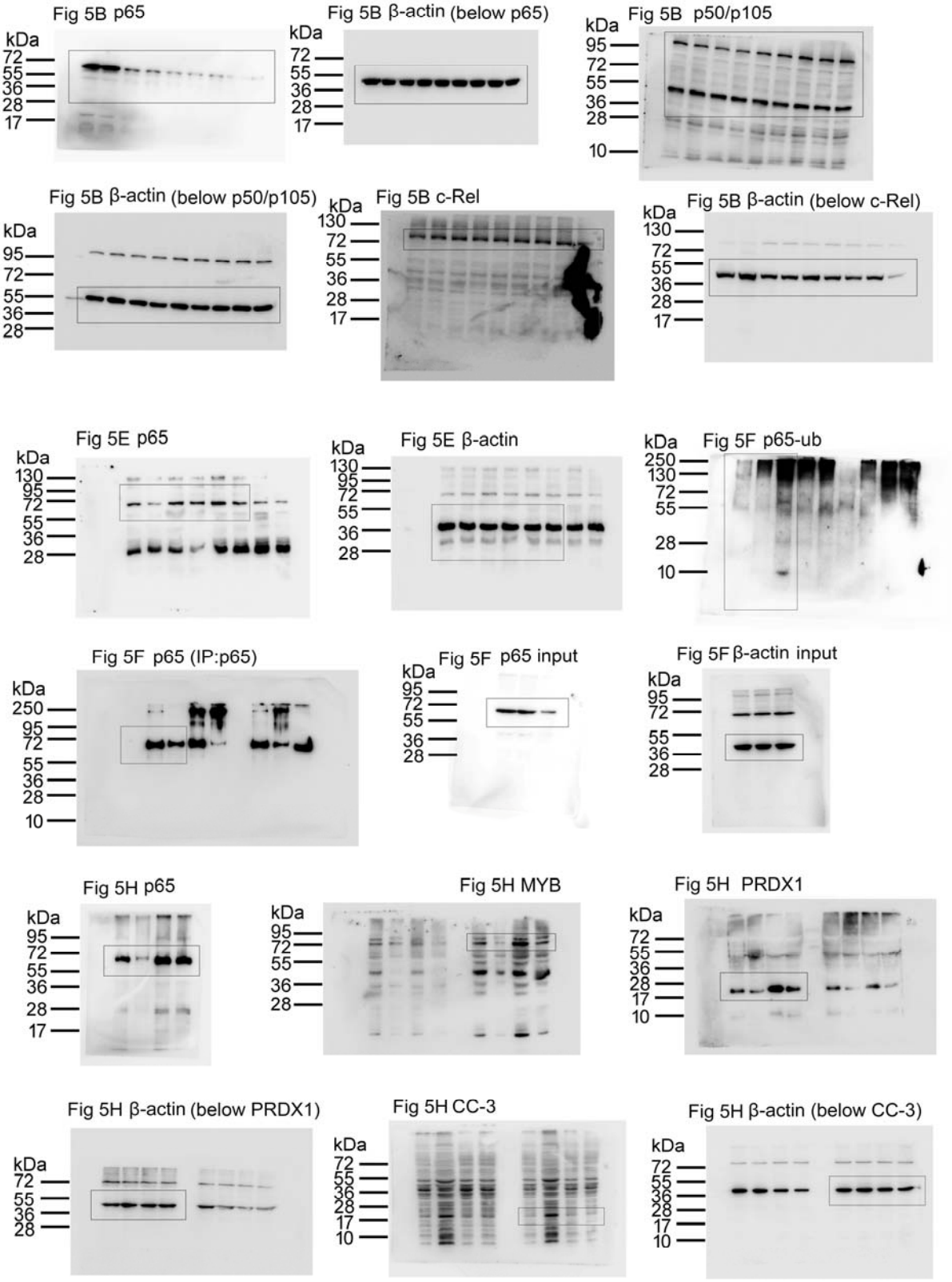

Figure 14 (Full blots: Fig 6A)

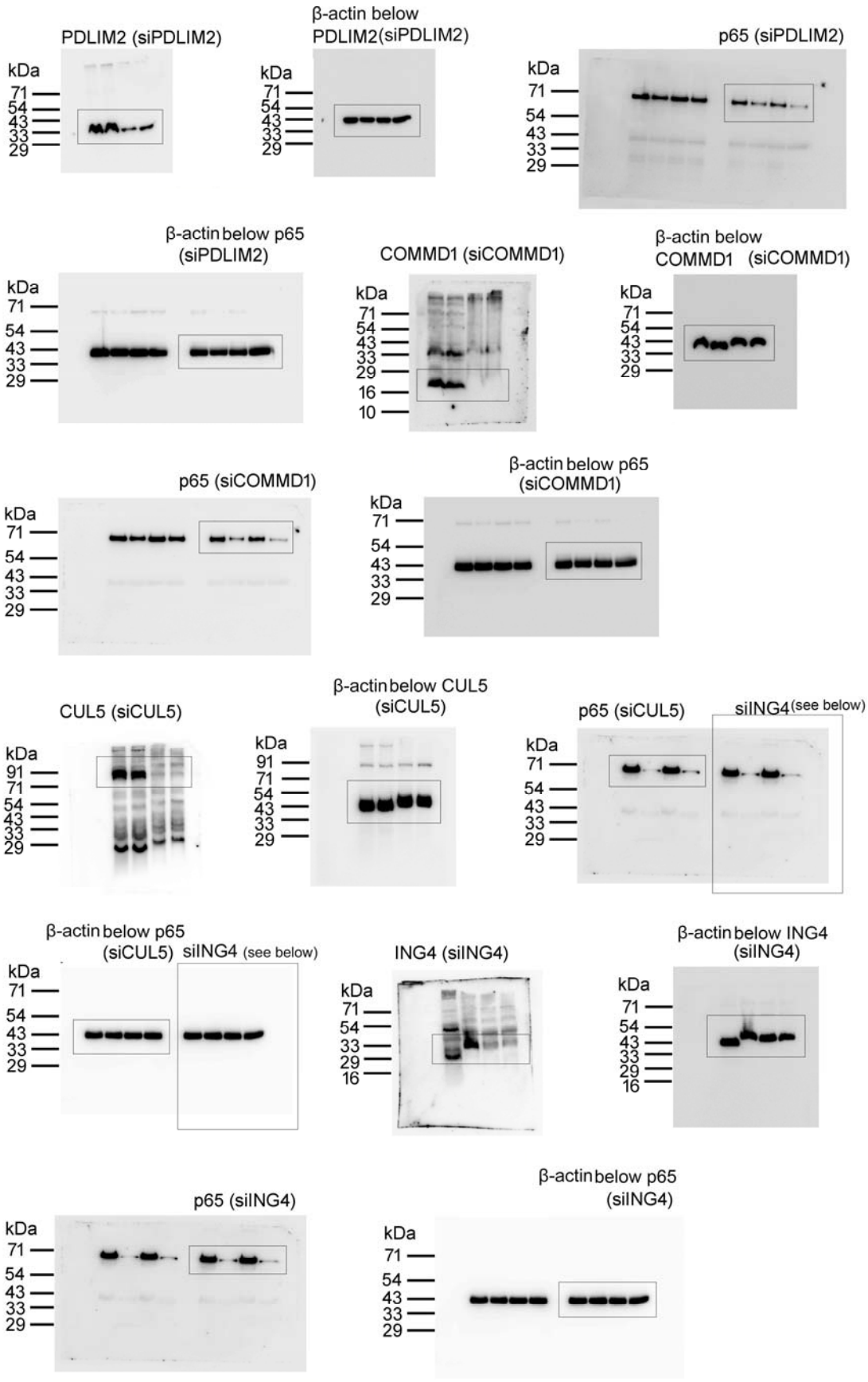

Figure S14 (Full blots: Fig 6B)

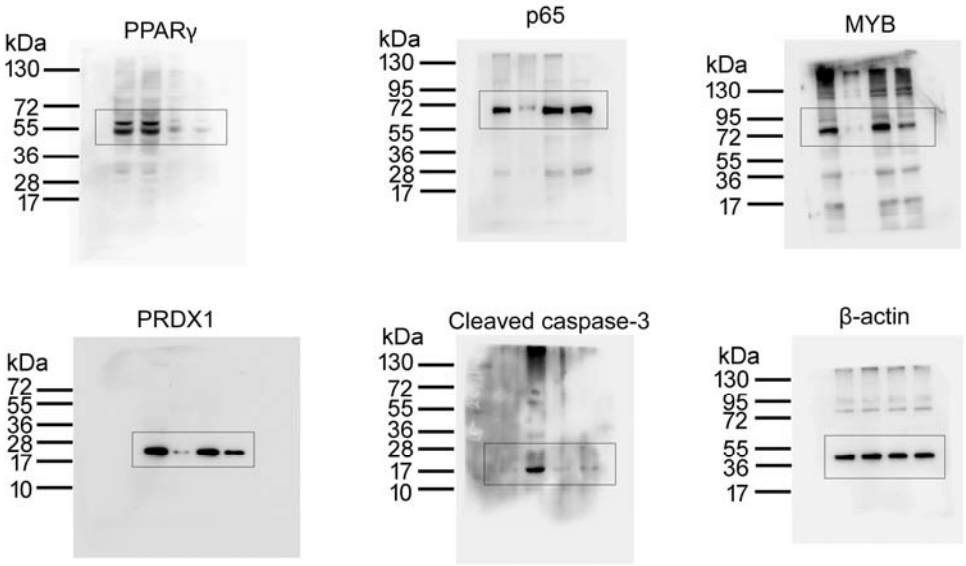

Figure S14 (Full blots: Fig 7)

Fig 7A STAT5

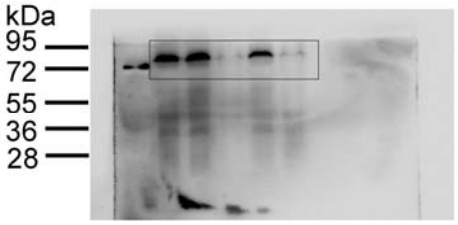

Fig 7A β-actin

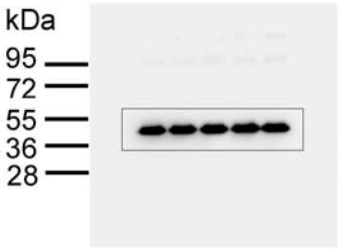

Fig 7B P-STAT5

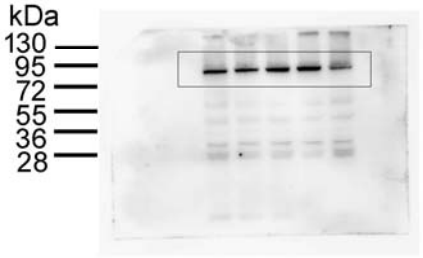

Fig 7B β-actin

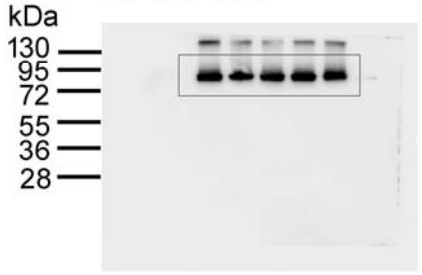

Fig 7D P-Crkl

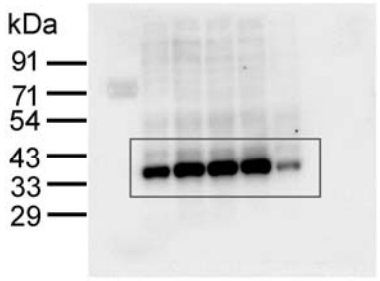

Fig 7D β-actin

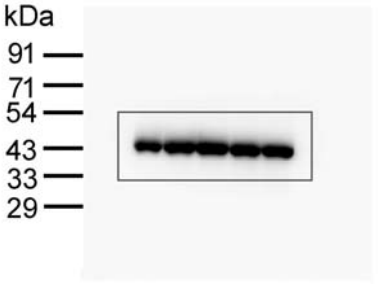

Fig 7D
P-BCR-ABL

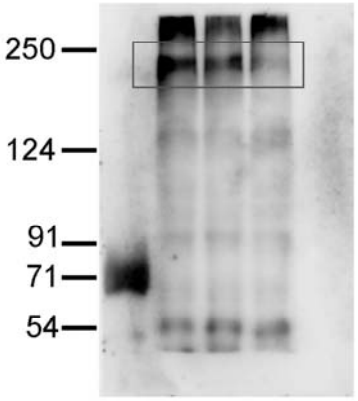

Fig 7D
BCR-ABL

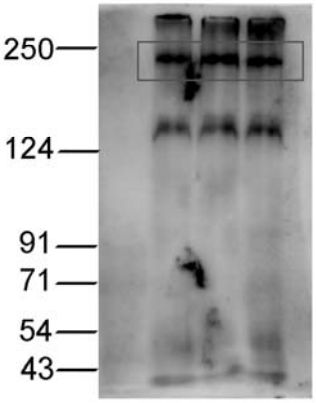

Figure S14 (Full blots: Fig S7)

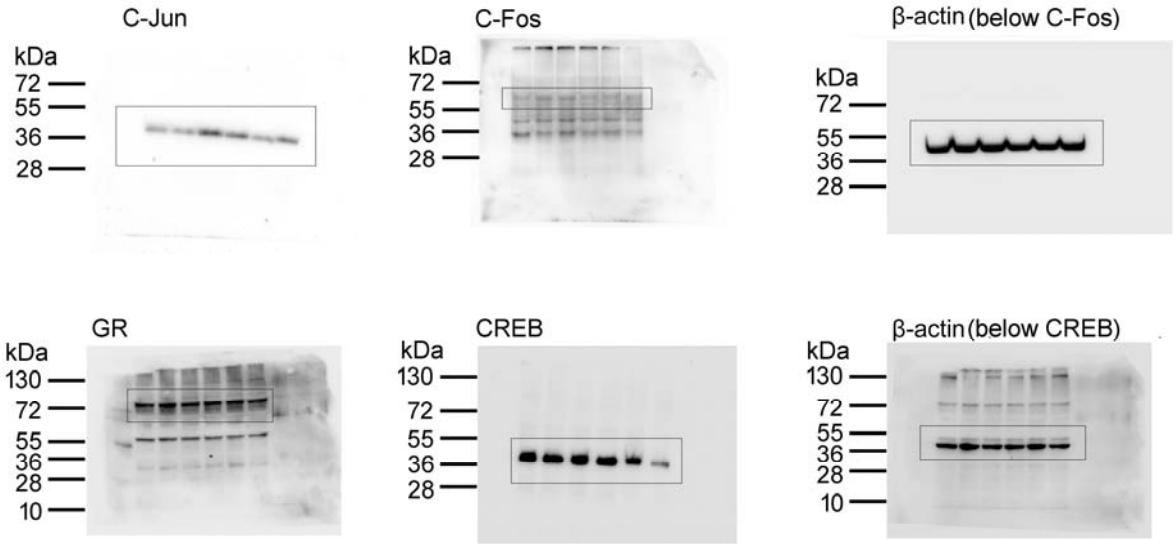

References

1. Dahle O, Andersen TO, Nordgard O, Matre V, Del Sal G, Gabrielsen OS. Transactivation properties of MYB are critically dependent on two SUMO-1 acceptor sites that are conjugated in a PIASy enhanced manner. Eur J Biochem. 2003;270(6):1338-1348.
2. Molvaersmyr AK, Saether T, Gilfillan S, et al. A SUMO-regulated activation function controls synergy of MYB through a repressor-activator switch leading to differential p300 recruitment. Nucleic Acids Res. 2010;38(15):4970-4984.
3. Watanabe A, Yoneda M, Ikeda F, Sugai A, Sato H, Kai C. Peroxiredoxin 1 is required for efficient transcription and replication of measles virus. J Virol. 2011;85(5):2247-2253.
4. Pochetti G, Godio C, Mitro N, et al. Insights into the mechanism of partial agonism: crystal structures of the peroxisome proliferator-activated receptor gamma ligand-binding domain in the complex with two enantiomeric ligands. J Biol Chem. 2007;282(23):17314-17324.
5. Bhargavan B, Singh D, Gautam AK, et al. Medicarpin, a legume phytoalexin, stimulates osteoblast differentiation and promotes peak bone mass achievement in rats: evidence for estrogen receptor beta-mediated osteogenic action of medicarpin. J Nutr Biochem. 2012;23(1):27-38.
6. Shiota M, Izumi H, Miyamoto N, et al. Ets regulates peroxiredoxin1 and 5 expressions through their interaction with the high-mobility group protein B1. Cancer Sci. 2008;99(10):1950-1959.
7. Singh AK, Joharapurkar AA, Khan MP, et al. Orally active osteoanabolic agent GTDF binds to adiponectin receptors, with a preference for AdipoR1, induces adiponectin-associated signaling, and improves metabolic health in a rodent model of diabetes. Diabetes. 2014;63(10):3530-3544.
8. Yadav M, Singh AK, Kumar H, et al. Epidermal growth factor receptor inhibitor cancer drug gefitinib modulates cell growth and differentiation of acute myeloid leukemia cells via histamine receptors. Biochim Biophys Acta. 2016;1860(10):2178-2190.